7

Measurement of High Voltages and Currents

In industrial testing and research laboratories, it is essential to measure the voltages and currents accurately, ensuring perfect safety to the personnel and equipment. Hence a person handling the equipment as well as the metering devices must be protected against overvoltages and also against any induced voltages due to stray coupling. Therefore, the location and layout of the devices are important. Secondly, linear extrapolation of the devices beyond their ranges are not valid for high voltage meters and measuring instruments, and they have to be calibrated for the full range. Electromagnetic interference is a serious problem in impulse voltage and current measurements, and it has to be avoided or minimized. Therefore, even though the principles of measurements may be same, the devices and instruments for measurement of high voltages and currents differ vastly from the low voltage and low current devices. Different devices used for high voltage measurements may be classified as in Tables 7.1 and 7.2.

7.1 MEASUREMENT OF HIGH DIRECT CURRENT VOLTAGES

Measurement of high d.c. voltages as in low voltage measurements, is generally accomplished by extension of meter range with a large series resistance. The net current in the meter is usually limited to one to ten microamperes for full-scale deflection. For very high voltages (1000 kV or more) problems arise due to large power dissipation, leakage currents and limitation of voltage stress per unit length, change in resistance due to temperature variations, etc. Hence, a resistance potential divider with an electrostatic voltmeter is sometimes better when high precision is needed. But potential dividers also suffer from the disadvantages stated above. Both series resistance meters and potential dividers cause current drain from the source. Generating voltmeters are high impedance devices and do not load the source. They provide complete isolation from the source voltage (high voltage) as they are not directly connected to the high voltage terminal and hence are safer. Spark gaps such as sphere gaps are gas discharge devices and give an accurate measure of the peak voltage. These are quite simple and do not require any specialized construction. But the measurement is affected by the atmospheric conditions like temperature, humidity, etc. and by the vicinity of earthed objects, as the electric field in the gap is affected by the presence of earthed objects. But sphere gap measurement of voltages is independent of the waveform and frequency.

Table 7.1 High voltage Measurbment Techniques

Type of voltage	Method or technique
(*a*) d.c. voltages	(*i*) Series resistance microammeter
	(*ii*) Resistance potential divider
	(*iii*) Generating voltmeters
	(*iv*) Sphere and other spark gaps
(*b*) a.c. voltages	(*i*) Series impedance ammeters
(power frequency)	(*ii*) Potential dividers (resistance or capacitance type)
	(*iii*) Potential transformers (electromagnetic or CVT)
	(*iv*) Electrostatic voltmeters
	(*v*) Sphere gaps
(c) a.c. high frequency voltages, impulse voltages, and other rapidly changing voltages	(*i*) Potential dividers with a cathode ray oscillograph (resistive or capacitive dividers) (*ii*) Peak voltmeters (*iii*) Sphere gaps

Table 7.2 High Current Measurement Techniques

Type of current	Device or technique
(*a*) Direct currents	(*i*) Resistive shunts with milliammeter
	(*ii*) Hall effect generators
	(*iii*) Magnetic links
(*b*) Alternating currents	(*i*) Resistive shunts
(Power frequency)	(*ii*) Electromagnetic current transformers
(*c*) High frequency a.c.,	(*i*) Resistive shunts
impulse and rapidly	(*ii*) Magnetic potentiometers or Rogowski coils
changing currents	(*iii*) Magnetic links
	(*iv*) Hall effect generators

7.1.1 High Ohmic Series Resistance with Microammeter

High d.c. voltages are usually measured by connecting a very high resistance (few hundreds of megaohms) in series with a microammeter as shown in Fig. 7.1. Only the current I flowing through the large calibrated resistance R is measured by the moving coil microammeter. The voltage of the source is given by

$$V = I R$$

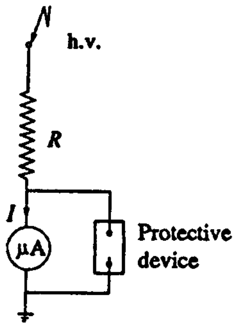

Fig. 7.1 Series resistance micrometer

The voltage drop in the meter is negligible, as the impedance of the meter is only few ohms compared to few hundred mega-ohms of the series resistance R. A protective device like a paper gap, a neon glow tube, or a zener diode with a suitable series resistance is connected across the meter as a protection against high voltages in case the series resistance R fails or flashes over. The ohmic value of the series resistance R is chosen such that a current of one to ten microamperes is allowed for full-scale deflection. The resistance is constructed from a large number of wire wound resistors in series. The voltage drop in each resistor element is chosen to avoid surface flashovers and discharges. A value of less than 5 kV/cm in air or less than 20 kV/cm in good oil is permissible. The resistor chain is provided with corona free terminations. The material for resistive elements is usually a carbon-alloy with temperature coefficient less than 10^{-4}/°C. Carbon and other metallic film resistors are also used. A resistance chain built with ±1% carbon resistors located in an airtight transformer oil filled P.V.C. tube, for 100 kV operation had very good temperature stability. The limitations in the series resistance design are:

(*i*) power dissipation and source loading,
(*ii*) temperature effects and long time stability,
(*iii*) voltage dependence of resistive elements, and
(*iv*) sensitivity to mechanical stresses.

Series resistance meters are built for 500 kV d.c. with an accuracy better than 0.2%.

7.1.2 Resistance Potential Dividers for d.c. Voltages

A resistance potential divider with an electrostatic or high impedance voltmeter is shown in Fig. 7.2. The influence of temperature and voltage on the elements is eliminated in the voltage divider arrangement. The high voltage magnitude is given by $[(R_1 + R_2)/R_2]v_2$, where v_2 is the d.c. voltage across the low voltage arm R_2. With sudden changes in voltage, such as switching operations, flashover of the test objects, or source short circuits, flashover or damage may occur to the divider elements due to the stray capacitance across the elements and due to ground capacitances. To avoid these transient voltages, voltage controlling capacitors are connected across the elements. A corona free termination is also necessary to avoid unnecessary discharges at high voltage ends. A series resistor with a parallel capacitor connection for linearization of transient potential distribution is shown in Fig. 7.3. Potential dividers are made with 0.05% accuracy up to 100 kV, with 0.1% accuracy up to 300 kV, and with better than 0.5% accuracy for 500 kV.

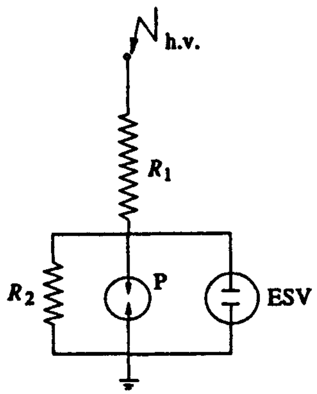

Fig. 7.2 Resistance potential divider with an electrostatic voltmeter

P — Protective device
ESV — Electrostatic volt-meter

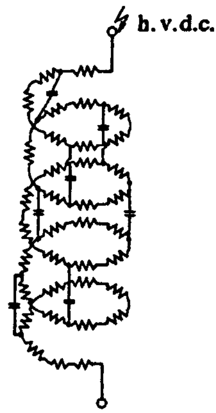

Fig. 7.3 Series resistor with parallel capacitors for potential linearization for transient voltages

7.1.3 Generating Voltmeters

High voltage measuring devices employ generating principle when source loading is prohibited (as with Van de Graaff generators, etc.) or when direct connection to the high voltage source is to be avoided. A generating voltmeter is a variable capacitor electrostatic voltage generator which generates current proportional to the applied external voltage. The device is driven by an external synchronous or constant speed motor and does not absorb power or energy from the voltage measuring source.

Principle of Operation

The charge stored in a capacitor of capacitance C is given by $q = CV$. If the capacitance of the capacitor varies with time when connected to the source of voltage V, the current through the capacitor,

$$i = \frac{dq}{dt} = V\frac{dC}{dt} + C\frac{dV}{dt} \tag{7.1}$$

For d.c. voltages $dV/dt = 0$. Hence,

$$i = \frac{dq}{dt} = V\frac{dC}{dt} \tag{7.2}$$

If the capacitance C varies between the limits C_0 and $(C_0 + C_m)$ sinusoidally as

$$C = C_0 + C_m \sin \omega t$$

the current i is

$$i = i_m \operatorname{cost} \omega t$$

where $$i_m = V C_m \omega$$

(i_m is the peak value of the current). The rms value of the current is given by:

$$i_{rms} = \frac{VC_m\omega}{\sqrt{2}} \tag{7.3}$$

For a constant angular frequency ω, the current is proportional to the applied voltage V. More often, the generated current is rectified and measured by a moving coil meter. Generating voltmeter can be used for a.c. voltage measurements also provided the angular frequency ω is the same or equal to half that of the supply frequency.

A generating voltmeter with a rotating cylinder consists of two exciting field electrodes and a rotating two pole armature driven by a synchronous motor at a constant speed n. The a.c. current flowing between the two halves of the armature is rectified by a commutator whose arithmetic mean may be calculated from:

$$i = \frac{n}{30}\Delta C\,V, \qquad \text{where } \Delta C = C_{max} - C_{min}$$

For a symmetric voltage $C_{min} = 0$. When the voltage is not symmetrical, one of the electrodes is grounded and C_{min} has a finite value. The factor of proportionality $\frac{n}{30}\cdot\Delta C$ is determined by calibration.

This device can be used for measuring a.c. voltages provided the speed of the drive-motor is half the frequency of the voltage to be measured. Thus a four-pole synchronous motor with 1500 rpm is suitable for 50 Hz. For peak value measurements, the phase angle of the motor must also be so adjusted that C_{max} and the crest value occur at the same instant.

Generating voltmeters employ rotating sectors or vanes for variation of capacitance. Figure 7.4 gives a schematic diagram of a generating voltmeter. The high voltage source is connected to a disc electrode S_3 which is kept at a fixed distance on the axis of the other low voltage electrodes S_0, S_1, and S_2. The rotor S_0 is driven at a constant speed by a synchronous motor at a suitable speed (1500, 1800, 3000, or 3600 rpm). The rotor vanes of S_0 cause periodic change in capacitance between the insulated disc S_2 and the h.v. electrode S_3. The shape and number of the vanes of S_0 and S_1 are so designed that they produce sinusoidal variation in the capacitance. The generated a.c. current through the resistance R is rectified and read by a moving coil instrument. An amplifier is needed, if the shunt capacitance is large or longer leads are used for connection to rectifier and meter. The instrument is calibrated using a potential divider or sphere gap. The meter scale is linear and its range can be extended

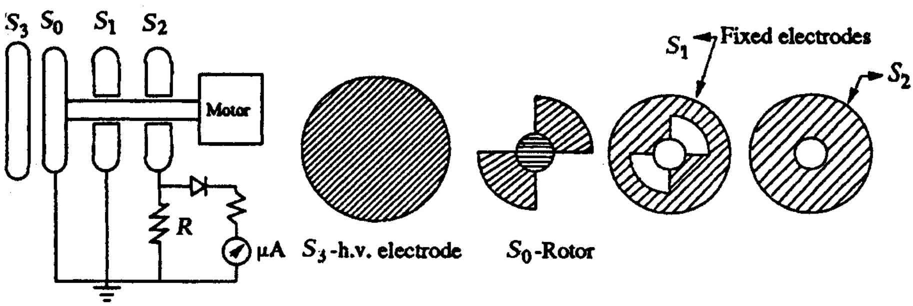

Fig. 7.4 Schematic diagram of a generating voltmeter (rotating vane type)

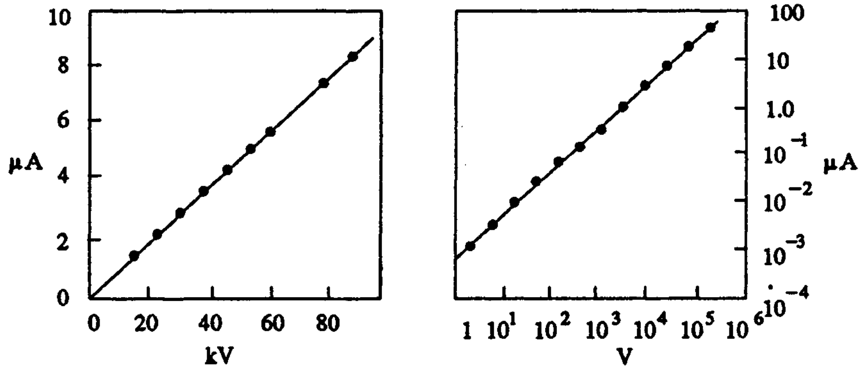

(a) Rotating cylinder type

(b) Rotating vane type

Fig. 7.5 Calibration curves for a generating voltmeter

by extrapolation. Typical calibration curves of a generating voltmeter are given in Figs. 7.5a and b.

Advantages of Generating Voltmeters

(*i*) No source loading by the meter,
(*ii*) no direct connection to high voltage electrode,
(*iii*) scale is linear and extension of range is easy, and
(*iv*) a very convenient instrument for electrostatic devices such as Van de Graaff generator and particle accelerators.

Limitations of Generating Voltmeters

(*i*) They require calibration,
(*ii*) careful construction is needed and is a cumbersome instrument requiring an auxiliary drive, and
(*iii*) disturbance in position and mounting of the electrodes make the calibration invalid.

7.1.4 Other Methods—Oscillating Spheroid

The period of oscillation of an oscillating spheroid in a uniform electric field is proportional to the applied electric field. This principle is made use of in measuring high d.c. voltages. The period of oscillation of a suspended spheroid between two electrodes with and without an electric field present is measured. If the frequency of the oscillation for small amplitudes is f and f_0 respectively, then the electric field

$$E \propto [f^2 - f_0^2]^{1/2}$$

and hence the applied voltage

$$V \propto [f^2 - f_0^2]^{1/2} \tag{7.4}$$

since $E = V/d$ (d being the gap separation between the electrodes). The proportionality constant can be determined from the dimensions of the spheroid or experimentally.

The uniform electric field is produced by employing two electrodes with a Bruce profile for a spacing of about 50 cm. One of the electrodes is earthed and the other is connected to a high voltage d.c. source. The spheroid is suspended at the centre of the electrodes in the axis of the electric field. The period of oscillation is measured using a telescope and stop watch. Instruments of this type are constructed for voltages up to 200 kV, and the accuracy is estimated to be ±0.1%. In Bruce's design, electrodes of 145 cm diameter with 45 cm spacing were used. An overall accuracy of ±0.03% was claimed up to a maximum voltage of 250 kV. Since this is a very complicated and time consuming method, it is not widely used. The useful range of the spheroidal voltmeter is limited by local discharges.

7.1.5 Measurement of Ripple Voltage in d.c. Systems

It has been discussed in the previous chapter that d.c. rectifier circuits contain ripple, which should be kept low (<< 3%). Ripple voltages are a.c. voltages of non-sinusoidal nature, and as such oscillographic measurement of these voltages is desirable. However, if a resistance potential divider is used along with an oscilloscope, the measurement of small values of the ripple δV will be inaccurate.

A simple method of measuring the ripple voltage is to use a capacitance-resistance (C-R) circuit and measure the varying component of the a.c. voltage by blocking the d.c. component. If V_1 is the d.c. source voltage with ripple (Fig. 7.6a) and V_2 is the voltage across the measuring resistance R, with C acting as the blocking capacitor, then

$$V_2(t) = V_1(t) - V_{\text{d.c.}} = \text{ripple voltage}$$

The condition to be satisfied here is $\omega CR >> 1$.

Measurement of Ripple with CRO

The detailed circuit arrangement used for this purpose is shown in Fig. 7.6b. Here, the capacitance 'C' is rated for the peak voltage. It is important that the switch 'S' be closed when the CRO is connected to the source so that the CRO input terminal does not receive any high voltage signal while 'C' is being charged. Further, C should be

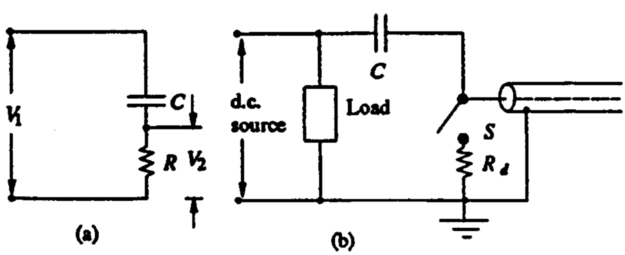

Fig. 7.6 Circuit arrangement for the measurement of ripple voltage

larger than the capacitance of the cable and the input capacitance of the *CRO*, taken together.

7.2 MEASUREMENT OF HIGH a.c. AND IMPULSE VOLTAGES: INTRODUCTION

Measurement of high a.c. voltages employ conventional methods like series impedance voltmeters, potential dividers, potential transformers, or electrostatic voltmeters. But their designs are different from those of low voltage meters, as the insulation design and source loading are the important criteria. When only peak value measurement is needed, peak voltmeters and sphere gaps can be used. Often, sphere gaps are used for calibration purposes. Impulse and high frequency a.c. measurements invariably use potential dividers with a cathode ray oscillograph for recording voltage waveforms. Sphere gaps are used when peak values of the voltage are only needed and also for calibration purposes.

7.2.1 Series Impedance Voltmeters

For power frequency a.c. measurements the series impedance may be a pure resistance or a reactance. Since resistances involve power losses, often a capacitor is preferred as a series reactance. Moreover, for high resistances, the variation of resistance with temperature is a problem, and the residual inductance of the resistance gives rise to an impedance different from its ohmic resistance. High resistance units for high voltages have stray capacitances and hence a unit resistance will have an equivalent circuit as shown in Fig. 7.7. At any frequency ω of the a.c. voltage, the impedance of the resistance R is

$$Z = \frac{R + j\omega L}{(1 - \omega^2 LC) + j\omega CR} \tag{7.5}$$

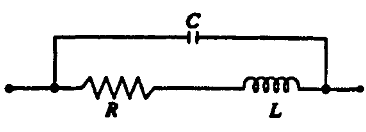

Fig. 7.7 Simplified lumped parameter equivalent circuit of a high ohmic resistance R

L — Residual inductance

C — Residual capacitance

If ωL and ωC are small compared to R,

$$Z \approx R\left[1 + j\left(\frac{\omega L}{R} - \omega CR\right)\right] \tag{7.6}$$

and the total phase angle is

$$\varphi \approx \left(\frac{\omega L}{R} - \omega CR\right) \tag{7.7}$$

This can be made zero and independent of frequency, if

$$L/C = R^2 \tag{7.8}$$

For extended and large dimensioned resistors, this equivalent circuit is not valid and each elemental resistor has to be approximated with this equivalent circuit. The entire resistor unit then has to be taken as a transmission line equivalent, for calculating the effective resistance. Also, the ground or stray capacitance of each element influences the current flowing in the unit, and the indication of the meter results in an error. The equivalent circuit of a high voltage resistor neglecting inductance and the circuit of compensated series resistor using guard and tuning resistors is shown in Figs. 7.8a and b respectively. Stray ground capacitance effects (refer Fig. 7.8b) can be removed by shielding the resistor R by a second surrounding spiral R_s, which shunts the actual resistor but does not contribute to the current through the instrument. By tuning the resistors R_a, the shielding resistor end potentials may be adjusted with respect to the actual measuring resistor so that the resulting compensation currents between the shield and the measuring resistors provide a minimum phase angle.

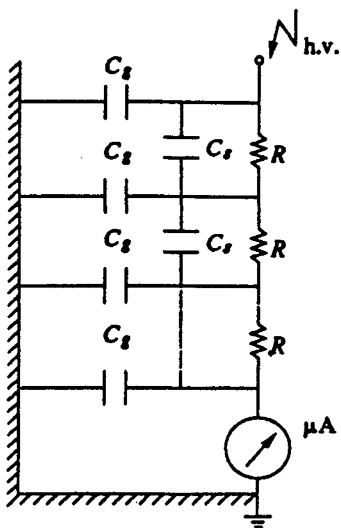

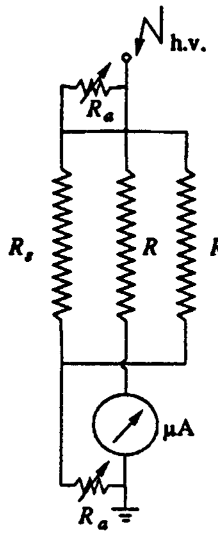

(a) Extended series resistance with inductance neglected

C_g — Stray capacitance to ground
C_s — Winding capacitance

(b) Series resistance with guard and tuning resistances

R — Series resistor
R_s — Guard resistor
R_a — Tuning resistor

Fig. 7.8 Extended series resistance for high a.c. voltage measurements

Series Capacitance Voltmeter

To avoid the drawbacks pointed out earlier, a series capacitor is used instead of a resistor for a.c. high voltage measurements. The schematic diagram is shown in Fig. 7.9. The current I_c through the meter is:

$$I_c = j\,\omega\,CV \tag{7.9}$$

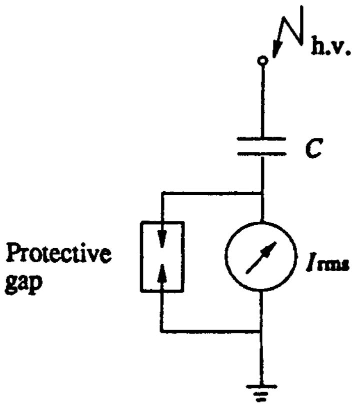

Fig. 7.9 Series capacitance with a milliammeter for measurement of high a.c. voltages

where, C = capacitance of the series capacitor,

ω = angular frequency, and

V = applied a.c. voltage.

If the a.c. voltage contains harmonics, error due to changes in series impedance occurs. The rms value of the voltage V with harmonics is given by

$$V = \sqrt{V_1^2 + V_2^2 + \dots V_n^2} \tag{7.10}$$

where V_1, V_2, ... V_n represent the rms value of the fundamental, second ... and nth harmonics.

The currents due to these harmonics are

$$\begin{aligned} I_1 &= \omega\,CV_1 \\ I_2 &= 2\,\omega\,CV_2, \dots, \text{and} \\ I_n &= n\,\omega\,CV_n \end{aligned} \tag{7.11}$$

Hence, the resultant rms current is:

$$I = \omega\,C\,(V_1^2 + 4V_2^2 + \dots + n^2V_n^2)^{1/2} \tag{7.12}$$

With a 10% fifth harmonic only, the current is 11.2% higher, and hence the error is 11.2% in the voltage measurement.

This method is not recommended when a.c. voltages are not pure sinusoidal waves but contain considerable harmonics.

Series capacitance voltmeters were used with cascade transformers for measuring rms values up to 1000 kV. The series capacitance was formed as a parallel plate capacitor between the high voltage terminal of the transformer and a ground plate suspended above it. A rectifier ammeter was used as an indicating instrument and was directly calibrated in high voltage rms value. The meter was usually a 0-100 μA moving coil meter and the over all error was about 2%.

7.2.2 Capacitance Potential Dividers and Capacitance Voltage Transformers

The errors due to harmonic voltages can be eliminated by the use of capacitive voltage dividers with an electrostatic voltmeter or a high impedance meter such as a V.T.V.M. If the meter is connected through a long cable, its capacitance has to be taken into account in calibration. Usually, a standard compressed air or gas condenser is used as C_1 (Fig. 7.10), and C_2 may be any large capacitor (mica, paper, or any low loss condenser). C_1 is a three terminal capacitor and is connected to C_2 through a shielded cable, and C_2 is completely shielded in a box to avoid stray capacitances. The applied voltage V_1 is given by

$$V_1 = V_2\left(\frac{C_1 + C_2 + C_m}{C_1}\right) \qquad (7.13)$$

where C_m is the capacitance of the meter and the connecting cable and the leads and V_2 is the meter reading.

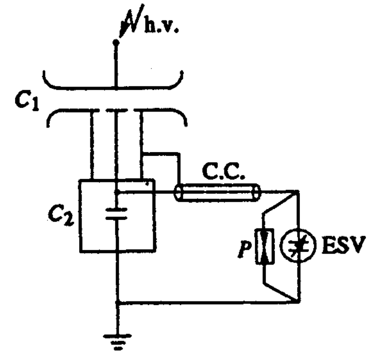

Fig. 7.10 Capacitance potential divider

C_1 — Standard compressed gas h.v. condenser
C_2 — Standard low voltage condenser
ESV — Electrostatic voltmeter
P — Protective gap
C.C. — Connecting cable

Capacitance Voltage Transformer—CVT

Capacitance divider with a suitable matching or isolating potential transformer tuned for resonance condition is often used in power systems for voltage measurements. This is often referred to as CVT. In contrast to simple capacitance divider which requires a high impedance meter like a V.T.V.M. or an electrostatic voltmeter, a CVT can be connected to a low impedance device like a wattmeter pressure coil or a relay coil. CVT can supply a load of a few VA. The schematic diagram of a CVT with its equivalent circuit is given in Fig. 7.11. C_1 is made of a few units of high voltage condensers, and the total capacitance will be around a few thousand picofarads as against a gas filled standard condenser of about 100 pF. A matching transformer is connected between the load or meter M and C_2. The transformer ratio is chosen on economic grounds, and the h.v. winding rating may be 10 to 30 kV with the l.v. winding rated from 100 to 500 V. The value of the tuning choke L is chosen to make the equivalent circuit of the CVT purely resistive or to bring resonance condition. This condition is satisfied when

$$\omega\,(L + L_T) = \frac{1}{\omega(C_1 + C_2)} \qquad (7.14)$$

where, L = inductance of the choke, and

L_T = equivalent inductance of the transformer referred to h.v. side.

The voltage V_2 (meter voltage) will be in phase with the input voltage V_1.

The phasor diagram of CVT under resonant conditions is shown in Fig. 7.11. The meter is taken as a resistive load, and X'_m is neglected. The voltage across the load referred to the divider side will be $V_2' = (I'_m R'_m)$ and $V_{C_2} = V_2' + I_m(R_e + X_e)$. It is clear from the phasor diagram that V_1 (input voltage) = $(V_{C_1} + V_{C_2})$ and is in phase

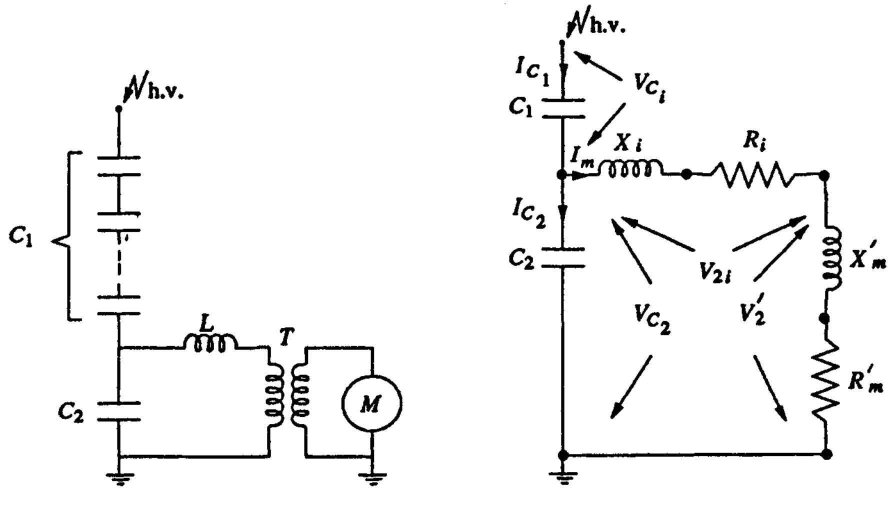

(a) Schematic representation (b) Equivalent circuit

Fig. 7.11 Capacitive voltage transformer (CVT)

with V_2', the voltage across the meter. R_e and X_e include the potential transformer resistance and leakage reactance. Under this condition, the voltage ratio becomes

$$a = (V_1/V_2) \simeq (V_{C_1} + V_{Ri} + V_2')/V_2' \qquad (7.15)$$

(neglecting the voltage drop $I_m \cdot X_e$ which is very small compared to the voltage V_{C_1}) where V_{Ri} is the voltage drop in the transformer and choke windings.

The advanges of a CVT are:

(*i*) simple design and easy installation,
(*ii*) can be used both as a voltage measuring device for meter and relaying purposes and also as a coupling condenser for power line carrier communication and relaying.
(*iii*) frequency independent voltage distribution along elements as against conventional magnetic potential transformers which require additional insulation design against surges, and
(*iv*) provides isolation between the high voltage terminal and low voltage metering.

The disadvantages of a CVT are:

(*i*) the voltage ratio is susceptible to temperature variations, and
(*ii*) the problem of inducing ferro-resonance in power systems.

Resistance Potential Dividers

Resistance potential dividers suffer from the same disadvantages as series resistance voltmeters for a.c. applications. Moreover, stray capacitances and inductances (Figs 7.7 and 7.8) associated with the resistances make them inaccurate, and compensation has to be provided. Hence, they are not generally used.

7.2.3 Potential Transformers (Magnetic Type)

Magnetic potential transformers are the oldest devices for a.c. measurements. They are simple in construction and can be designed for any voltage. For very high voltages, cascading of the transformers is possible. The voltage ratio is:

$$\frac{V_1}{V_2} = a = \frac{N_1}{N_2} \qquad (7.16)$$

where V_1 and V_2 are the primary and secondary voltages, and N_1 and N_2 are the respective turns in the windings.

These devices suffer from the ratio and phase angle errors caused by the magnetizing and leakage impedances of the transformer windings. The errors are compensated by adjusting the turns ratio with the tappings on the high voltage side under load conditions. Potential transformers (PT) do not permit fast rising transient or high frequency voltages along with the normal supply frequency, but harmonic voltages are usually measured with sufficient accuracy. With high voltage testing transformers, no separate potential transformer is used, but a PT winding is incorporated with the high voltage windings of the testing transformer.

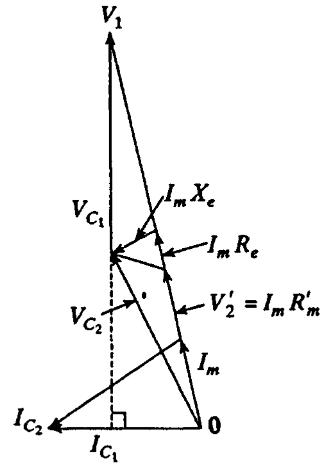

Fig. 7.12 Phasor diagram of a CVT under resonance or tuned condition, Z_m is taken to be equal to resistance R_m

With test objects like insulators, cables, etc. which are capacitive in nature, a voltage rise occurs on load with the testing transformer, and the potential transformer winding gives voltage values less than the actual voltages applied to the test object. If the percentage impedance of the testing transformer is known, the following correction can be applied to the voltage measured by the PT winding of the transformer.

$$V_2 = V_{20}(1 + 0.01\, v_x C/C_N) \qquad (7.17)$$

where, V_{20} = open circuit voltage of the PT winding,
C_N = load capacitance used for testing,
C = test object capacitance ($C << C_N$), and
v_x = % reactance drop in the transformer.

7.2.4 Electrostatic Voltmeters

Principle

In electrostatic fields, the attractive force between the electrodes of a parallel plate condenser is given by

$$F = \left|\frac{-\delta W_s}{dS}\right| = \left|\frac{\delta}{\delta S}\left(\tfrac{1}{2}CV^2\right)\right| = \left|\tfrac{1}{2}V^2\frac{\delta C}{\delta S}\right|$$

$$= \tfrac{1}{2}\varepsilon_0 V^2 \frac{A}{s^2} = \tfrac{1}{2}\varepsilon_0 A\left(\frac{V}{s}\right)^2 \tag{7.18}$$

where,
V = applied voltage between plates,
C = capacitance between the plates,
A = area of cross-section of the plates,
s = separation between the plates,
ε_0 = permittivity of the medium (air or free space), and
W_s = work done in displacing a plate

When one of the electrodes is free to move, the force on the plate can be measured by controlling it by a spring or balancing it with a counter weight. For high voltage measurements, a small displacement of one of the electrodes by a fraction of a millimetre to a few millimetres is usually sufficient for voltage measurements. As the force is proportional to the square of the applied voltage, the measurement can be made for a.c. or d.c. voltages.

Construction

Electrostatic voltmeters are made with parallel plate configuration using guard rings to avoid corona and field fringing at the edges. An absolute voltmeter is made by balancing the plate with a counter weight and is calibrated in terms of a small weight. Usually the electrostatic voltmeters have a small capacitance (5 to 50 pF) and high insulation resistance ($R \geq 10^{13}\ \Omega$). Hence they are considered as devices with high input impedance. The upper frequency limit for a.c. applications is determined from the following considerations:

(*i*) natural frequency of the moving system,
(*ii*) resonant frequency of the lead and stray inductances with meter capacitance, and
(*iii*) the R-C behaviour of the retaining or control spring (due to the frictional resistance and elastance).

An upper frequency limit of about one MHz is achieved in careful designs. The accuracy for a.c. voltage measurements is better than ±0.25%, and for d.c. voltage measurements it may be ±0.1% or less.

The schematic diagram of an absolute electrostatic voltmeter or electrometer is given in Fig. 7.13. It consists of parallel plane disc type electrodes separated by a small distance. The moving electrode is surrounded by a fixed guard ring to make the field uniform in the central region. In order to measure the given voltage with precision, the disc diameter is to be increased, and the gap distance is to be made less. The limitation on the gap distance is the safe working stress (V/s) allowed in air which is normally 5 kV/cm or less. The main difference between several forms of voltmeters lies in the manner in which the restoring force is obtained. For conventional versions of meters, a simple spring control is used, which actuates a pointer to move on the scale of the instruments. In more versatile instruments, only small movements of the moving electrodes is allowed, and the movement is amplified through optical means (lamp and scale arrangement as used with moving coil galvanometers). Two air vane dampers are used to reduce vibrational tendencies in the moving system, and the

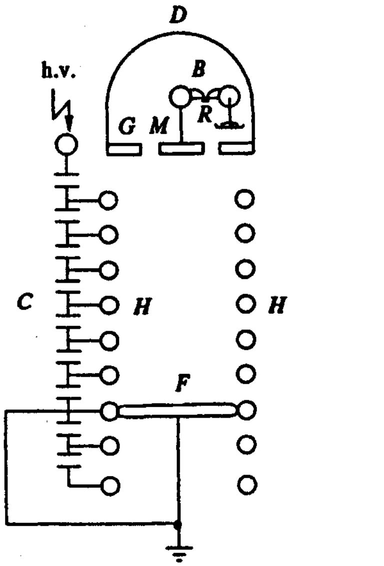

(a) Absolute electrostatic voltmeter

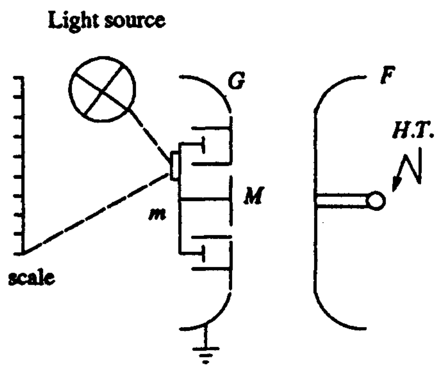

m — mirror
(b) Light beam arrangement

M — Mounting plate
G — Guard plate
F — Fixed plate
H — Guard hoops or rings
B — Balance
C — Capacitance divider
D — Dome
R — Balancing weight

Fig. 7.13 Electrostatic voltmeter

elongation of the spring is kept minimum to avoid field disturbances. The range of the instrument is easily changed by changing the gap separation so that V/s or electric stress is the same for the maximum value in any range. Multi-range instruments are constructed for 600 kV rms and above.

The constructional details of an absolute electrostatic voltmeter is given in Fig. 7.13a. The control torque is provided by a balancing weight. The moving disc M forms the central core of the guard ring G which is of the same diameter as the fixed plate F. The cap D encloses a sensitive balance B, one arm of which carries the suspension of the moving disc. The balance beam carries a mirror which reflects a beam of light. The movement of the disc is thereby magnified. As the spacing between the two electrodes is large, the uniformity of the electric field is maintained by the guard rings H which surround the space between the discs F and M. The guard rings H are maintained at a constant potential in space by a capacitance divider ensuring a uniform special potential distribution.

Some instruments are constructed in an enclosed structure containing compressed air, carbon dioxide, or nitrogen. The gas pressure may be of the order of 15 atm. Working stresses as high as 100 kV/cm may be used in an electrostatic meter in vacuum. With compressed gas or vacuum as medium, the meter is compact and much smaller in size.

7.2.5 Peak Reading a.c. Voltmeters

In some occasions, the peak value of an a.c. waveform is more important. This is necessary to obtain the maximum dielectric strength of insulating solids, etc. When the waveform is not sinusoidal, rms value of the voltage multiplied by $\sqrt{2}$ is not correct. Hence a separate peak value instrument is desirable in high voltage applications.

Series Capacitor Peak Voltmeter

When a capacitor is connected to a sinusoidal voltage source, the charging current $i_0 = C \int_0 v dt = j \omega CV$ where V is the rms value of the voltage and ω is the angular frequency. If a half wave rectifier is used, the arithmetic mean of the rectifier current is proportional to the peak value of the a.c. voltage. The schematic diagram of the circuit arrangement is shown in Fig. 7.14. The d.c. meter reading is proportional to the peak value of the value V_m or

$$V_m = \frac{I}{2\pi fC}$$

where I is the d.c. current read by the meter and C is the capacitance of the capacitor. This method is known as the Chubb-Frotscue method for peak voltage measurement.

The diode D_1 is used to rectify the a.c. current in one half cycle while D_2 by-passes in the other half cycle. This arrangement is suitable only for positive or negative half

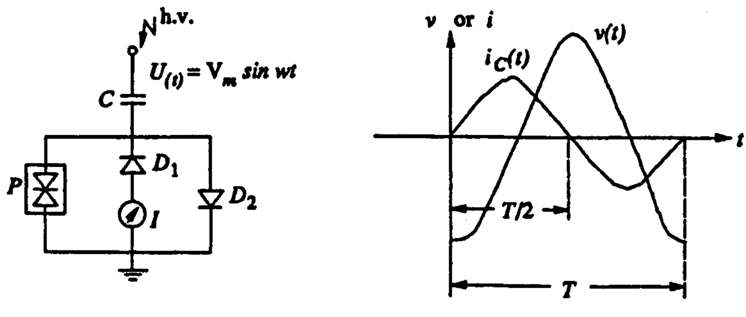

Fig. 7.14 Peak voltmeter with a series capacitor

C — Capacitor
D_1, D_2 — Diodes
P — Protective device
I — Indicating meter (rectified current indicated)

$v(t)$ — Voltage waveform
$I_c(t)$ — Capacitor current waveform
T — Period

cycles and hence is valid only when both half cycles are symmetrical and equal. This method is not suitable when the voltage waveform is not sinusoidal but contains more than one peak or maximum as shown in Fig. 7.14. The charging current through the capacitor changes its polarity within one half cycle itself. The shaded areas in Fig. 7.15 give the reverse current in any one of the half cycles and the current within that period subtracts from the net current. Hence the reading of the meter will be less and is not proportional to V_m as the current flowing during the intervals $(t_1 - t_2)$ etc. will not be included in the mean value. The 'second' or the false maxima is easily spotted out by observing the waveform of the charging current on an oscilloscope. Under normal conditions with a.c. testing, such waveforms do not occur and as such do not give rise to errors. But pre-discharge currents within the test circuits cause very short duration voltage drops which may introduce errors. This problem can also be overcome by using a resistance R in series with capacitor C such that $CR << 1/\omega$ for 50 Hz application. The error due to the resistance is

$$\frac{\Delta V}{V} = \frac{V - V_m}{V} = \left(1 - \frac{1}{1 + \omega^2 C^2 R^2}\right) \tag{7.19}$$

where, $V =$ actual value, and

$V_m =$ measured value

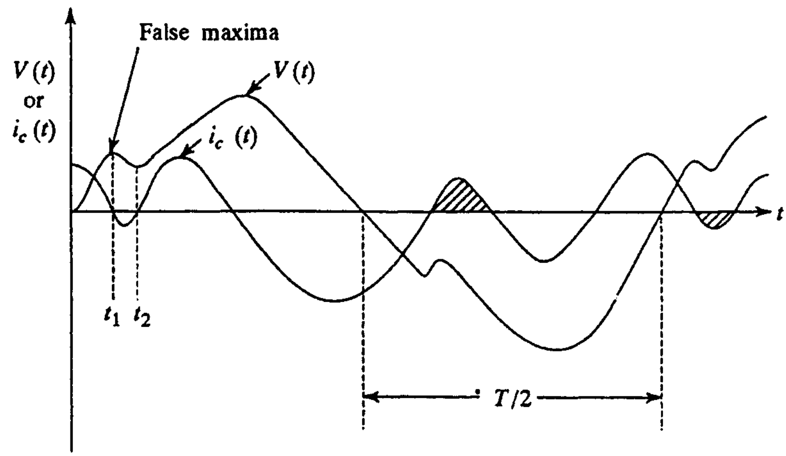

Fig. 7.15 Voltage waveform with harmonic content showing false maxima

In determining the error, the actual value of the angular frequency ω has to be determined.

The different sources that contribute to the error are

(*i*) the effective value of the capacitance being different from the measured value of C

(*ii*) imperfect rectifiers which allow small reverse currents

(*iii*) non-sinusoidal voltage waveforms with more than one peak or maxima per half cycle

(*iv*) deviation of the frequency from that of the value used for calibration

As such, this method in its basic form is not suitable for waveforms with more than one peak in each half cycle.

A digital peak reading meter for voltage measurements is shown in Fig. 7.16. Instead of directly measuring the rectified charging current, a proportional analog voltage signal is derived which is then converted into a proportional medium frequency, f_m. The frequency ratio f_m/f is measured with a gate circuit controlled by the a.c. power frequency (f) and a counter that opens for an adjustable number of periods $\Delta t = p/f$. During this interval, the number of impulses counted, n, is

$$n = f_m \cdot \Delta t = p \cdot \frac{f_m}{f} = 2pCV_m AR \tag{7.20}$$

where p is a constant of the instrument and A represents the conversion factor of the a.c. to d.c. converter. $A = f_m/(R\ i_m)$; i_m is the rectified current through resistance R. An immediate reading of the voltage in kV can be obtained by suitable choice of the parameters R and the number of periods p. The total estimated error in this instrument was less than 0.35%. Conventional instruments of this type are available with less than 2% error.

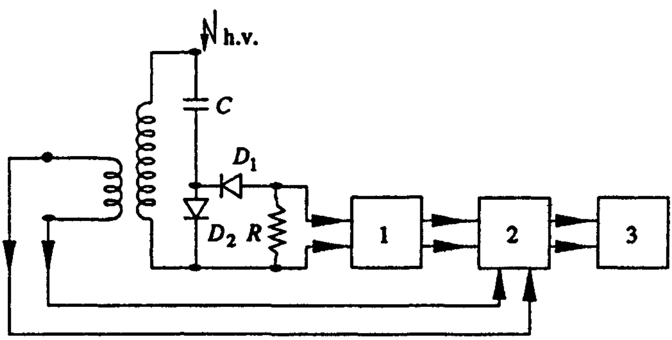

C — Series capacitor
D_1, D_2 — Diodes
R — Input resistor

1 — Voltage to frequency converter
2 — Gate circuit
3 — Read out counter (indicator)

Fig. 7.16 Digital peak voltmeter

Peak Voltmeters with Potential Dividers

Peak voltmeters using capacitance dividers designed by Bowlder *et al.*, are shown in Fig. 7.17a. The voltage across C_2 is made use of in charging the storage capacitor C_s. R_d is a discharge resistor employed to permit variation of V_m whenever V_2 is reduced. C_s is charged to a voltage proportional to the peak value to be measured. The indicating meter is either an electrostatic voltmeter or a high impedance V.T.V.M. The discharge time constant C_sR_d is designed to be about 1 to 10 s. This gives rise to a discharge error which depends on the frequency of the supply voltage. To compensate for the charging and discharging errors due to the resistances, the circuit is modified as shown in Fig. 7.17b. Measurement of the average peak is done by a microameter. Rabus' modification to compensate the charging errors is given in Fig. 7.17c.

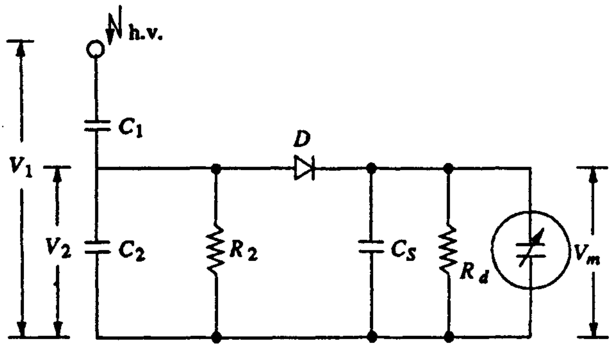

Fig. 7.17a Peak voltmeter with a capacitor potential divider and electrostatic voltmeter

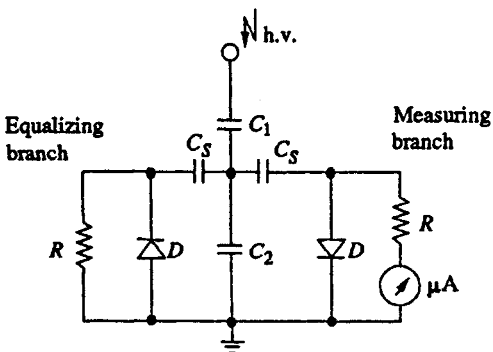

Fig. 7.17b Peak voltmeter as modified by Haefeely (ref. 19)

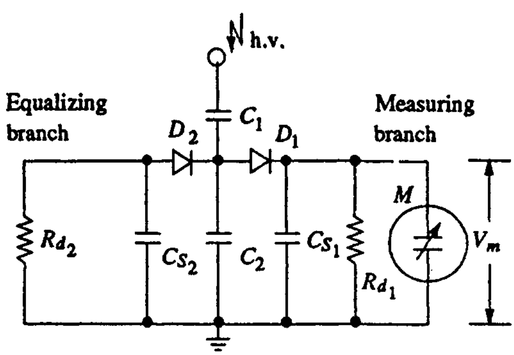

Rabus (ref. 20)

M — Electrostatic voltmeter or V.T.V.M. of high impedance

C_{S_2} — C_{S_1} + C meter

R_{d_2} — R_{d_1}

Fig. 7.17c Peak voltmeter with equalizing branch as designed by Rabus

7.2.6 Spark Gaps for Measurement of High d.c., a.c. and Impulse Voltages (Peak Values)

A uniform field spark gap will always have a sparkover voltage within a known tolerance under constant atmospheric conditions. Hence a spark gap can be used for measurement of the peak value of the voltage, if the gap distance is known. A sparkover voltage of 30 kV (peak) at 1 cm spacing in air at 20°C and 760 torr pressure occurs for a sphere gap or any uniform field gap. But experience has shown that these measurements are reliable only for certain gap configurations. Normally, only sphere gaps are used for voltage measurements. In certain cases uniform field gaps and rod gaps are also used, but their accuracy is less. The spark gap breakdown, especially the sphere gap breakdown, is independent of the voltage waveform and hence is highly suitable for all types of waveforms from d.c. to impulse voltages of short rise times (rise time ≥ 0.5 μ s). As such, sphere gaps can be used for radio frequency a.c. voltage peak measurements also (up to 1 MHz).

Sphere Gap Measurements

Sphere gaps can be arranged either (*i*) vertically with lower sphere grounded, or (*ii*) horizontally with both spheres connected to the source voltage or one sphere grounded. In horizontal configurations, it is generally arranged such that both spheres are symmetrically at high voltage above the ground. The two spheres used are identical in size and shape. The schematic arrangement is shown in Figs. 7.18a and 7.18b. The voltage to be measured is applied between the two spheres and the distance

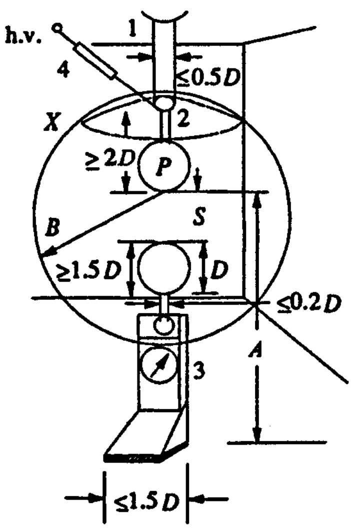

1 — Insulator support
2 — Sphere shank
3 — Operating gear and motor for changing gap distance
4 — H.V. connection
P — Sparking point
D — Diameter of the sphere
S — Spacing
A — Height of *P* above earth
B — Radius of the clearance from external structures
X — High voltage lead should not pass through this plane within a distance *B* from *P*

(a) Vertical arrangement of sphere gap

Fig. 7.18a Sphere gap for voltage measurement

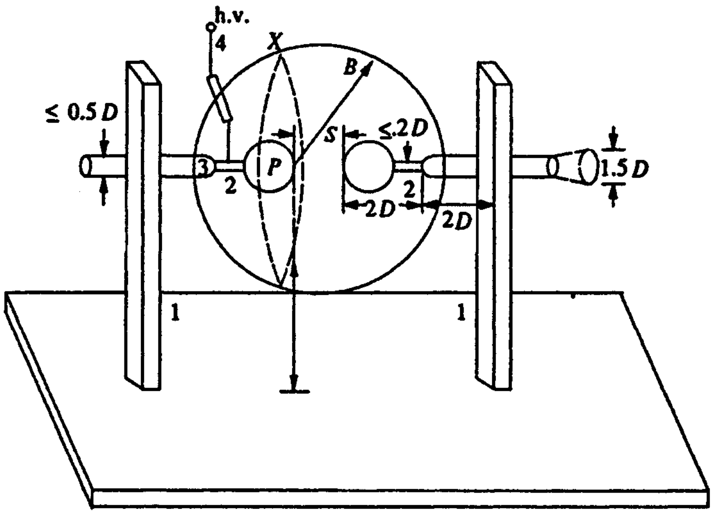

(b)

Fig. 7.18b Horizontal arrangement of sphere gap (Legend as in Fig. 7.18a)

or spacing S between them gives a measure of the sparkover voltage. A series resistance is usually connected between the source and the sphere gap to (*i*) limit the breakdown current, and (*ii*) to suppress unwanted oscillations in the source voltage when breakdown occurs (in case of impulse voltages). The value of the series resistance may vary from 100 to 1000 kilo ohms for a.c. or d.c. voltages and not more than 500 Ω in the case of impulse voltages.

In the case of a.c. peak value and d.c. voltage measurements, the applied voltage is uniformly increased until sparkover occurs in the gap. Generally, a mean of about five breakdown values is taken when they agree to within ±3%.

In the case of impulse voltages, to obtain 50% flashover voltage, two voltage limits, differing by not more than 2% are set such that on application of lower limit value either 2 or 4 flashovers take place and on application of upper limit value 8 or 6 flashovers take place respectively. The mean of these two limits is taken as 50% flashover voltage. In any case, a preliminary sparkover voltage measurement is to be made before actual measurements are made.

The flashover voltage for various gap distances and standard diameters of the spheres used are given in Tables 7.3 and 7.4 respectively. The values of sparkover voltages are specified in BS : 358, IEC Publication 52 of 1960 and IS : 1876 of 1962. The clearances necessary are shown in Figs. 7.18a and 7.18b for measurements to be within ±3%. The values of A and B indicated in the above figures are given in Table 7.5.

Table 7.3 Peak value of sparkover voltage in kV for a.c., d.c. voltages of either polarity, and for full negative standard impulse voltages (one sphere earthed) (a) and positive polarity impulse voltages and impulse voltages with long tails (b) at temperature: 25°C and pressure: 760 torr

Gap spacing (cm)	Sphere diameter (cm)															
	5		10		15		25		50		100		150		200	
	A	B	A	B	A	B	A	B	A	B	A	B	A	B	A	B
0.5	17.4	17.4	16.9	16.8	16.9	16.9										
1.0	32.0	32.0	31.7	31.7	31.4	31.4	31.2	31.4								
1.5	44.7	45.5	44.7	45.1	44.7	45.1	44.7	44.7								
2.0	57.5	58.0	58.0	58.0	58.0	58.0	58.0	58.0								
2.5			71.5	71.5	71.5	71.5	71.5	71.5	71.5	71.5						
3.0			85.0	85.0	85.0	85.0	85.0	85.0	85.0	85.0						
3.5			95.5	96.0	97.0	97.0	97.0	97.0	97.0	97.0						
4.0			106.0	108.0	108.0	110.0	110.0	110.0	110.0	110.0						
5.0			(123.0)	(127.0)	127.0	132.0	135.0	136.0	136.0	136.0						
7.5					(181.0)	(187.0)	195.0	196.0	199.0	199.0						
10.0							257	268	259	259	262	262	262	262	262	262
12.5							277	294	315	317						
15.0							(309)	(331)	367	374	383	384	384	384	384	384
17.5							(336)	(362)	413	425						
20.0									452	472	500	500	500	500	500	500
25.0									520	545	605	610				
30.0									(575)	(610)	700	715	730	735	735	740
35.0									(725)	(755)	785	800				
40.0											862	885	940	950	960	965
45.0											925	965				
50.0											1000	1020	1110	1130	1160	1170
75.0											(1210)	(1260)	1420	1460	1510	1590
100.0															1870	1900

Table 7.4 Sphere gap sparkover voltages in kV (peak) in air for a.c., d.c., and impulse voltage of either polarity for symmetrical sphere gaps at temperature: 20°c and pressure: 760 torr

Gap spacing (cm)	Sphere diameter (cm) 5	10	15	25	50	100	150	200	Remarks
0.5	17.5	16.9	16.5						For spacings less than 0.5 D, the accuracy is ± 3% and for spacings ≥ 0.5 D, the accuracy is ± 5%.
1.0	32.2	31.6	31.3	31.0					
1.5	46.1	45.8	45.5	45.0					
2.0	58.3	59.3	59.2	59.0					
2.5	69.4	72.4	72.9	73.0					
3.0	(79.3)	84.9	85.8	86.0					
4.0		107.0	111.0	113.0	112.0				
5.0		128.0	134.0	138.0	138.0	137.0	137.0	137.0	
8.0		(177)	194.0	207.0	214.0				
10.0				248.0	263.0	266.0	267.0	267.0	
12.0				286.0	309.0				
14.0				320.0	353.0				
16.0				352.0	394.0				
18.0					452.0				
20.0					495.0	504.0	511.0	511.0	
25.0					558.0	613.0	628.0	632.0	
30.0						744.0	741.0	746.0	
35.0						812.0	848.0	860.0	
40.0						902.0	950.0	972.0	
50.0						1070.0	1140.0	1180.0	
60.0						(1210)	1320.0	1380.0	
70.0							1490.0	1560.0	
80.0							(1640)	1730.0	
90.0								1900.0	
100.0								2050.0	

Sphere Gap Construction and Assembly

Sphere gaps are made with two metal spheres of identical diameters D with their shanks, operating gear, and insulator supports (Fig. 7.18a or b). Spheres are generally made of copper, brass, or aluminium; the latter is used due to low cost. The standard diameters for the spheres are 2, 5, 6.25, 10, 12.5, 15, 25, 50, 75, 100, 150, and 200 cm. The spacing is so designed and chosen such that flashover occurs near the sparking point P. The spheres are carefully designed and fabricated so that their surfaces are smooth and the curvature is uniform. The radius of curvature measured with a spherometer at various points over an area enclosed by a circle of 0.3 D around the sparking point should not differ by more than ±2% of the nominal value. The surface of the sphere should be free from dust, grease, or any other coating. The surface should be maintained clean but need not be polished. If excessive pitting occurs due to repeated sparkovers, they should be smoothened. The dimensions of the shanks used, the grading ring used (if necessary) with spheres, the ground clearances, etc. should follow the values indicated in Figs. 7.18a and 7.18b and Table 7.5. The high voltage conductor should be arranged such that it does not affect the field configuration. Series resistance connected should be outside the shanks at a distance $2D$ away from the high voltage sphere or the sparking point P.

Irradiation of sphere gap is needed when measurements of voltages less than 50 kV are made with sphere gaps of 10 cm diameter or less. The irradiation may be obtained from a quartz tube mercury vapour lamp of 40 W rating. The lamp should be at a distance B or more as indicated in Table 7.5.

Table 7.5 Clearances for Sphere Gaps

	Value of A		Value of
D (cm)	Max	Min	B (min)
up to 6.25	7 D	9 D	14S
10 to 15	6 D	8 D	12S
25	5 D	7 D	10S
50	4 D	6 D	8S
100	3.5 D	5 D	7S
150	3 D	4 D	6S
200	3 D	4 D	6S

A and B are clearances as shown in Figs. 7.18a and 7.18b.
D = diameter of the sphere; S = spacing of the gap; and $S/D \leq$ 0.5.

Factors Influencing the Sparkover Voltage of Sphere Gaps

Various factors that affect the sparkover voltage of a sphere gap are:

(*i*) nearby earthed objects,
(*ii*) atmospheric conditions and humidity,
(*iii*) irradiation, and
(*iv*) polarity and rise time of voltage waveforms.

Detailed investigations of the above factors have been made and analysed by Craggs and Meek[1], Kuffel and Abdullah[2], Kuffel[15], Davis and Boulder[16], and several other investigators. Only a few important factors are presented here.

(i) Effect of nearby earthed objects

The effect of nearby earthed objects was investigated by Kuffel[14] by enclosing the earthed sphere inside an earthed cylinder. It was observed that the sparkover voltage is reduced. The reduction was observed to be

$$\Delta V = m \log (B/D) + C \tag{7.21}$$

where, ΔV = percentage reduction,
B = diameter of earthed enclosing cylinder,
D = diameter of the spheres,
S = spacing, and m and C are constants.

The reduction was less than 2% for $S/D \leq 0.5$ and $B/D \geq 0.8$. Even for $S/D \approx 1.0$ and $B/D \geq 1.0$ the reduction was only 3%. Hence, if the specifications regarding the clearances are closely observed the error is within the tolerances and accuracy specified. The variation of breakdown voltage with A/D ratio is given in Figs. 7.19a and b for a 50 cm sphere gap. The reduction in voltage is within the accuracy limits, if S/D is kept less than 0.6. A in the above ratio A/D is the distance from sparking point to horizontal ground plane (also shown in Fig. 7.19).

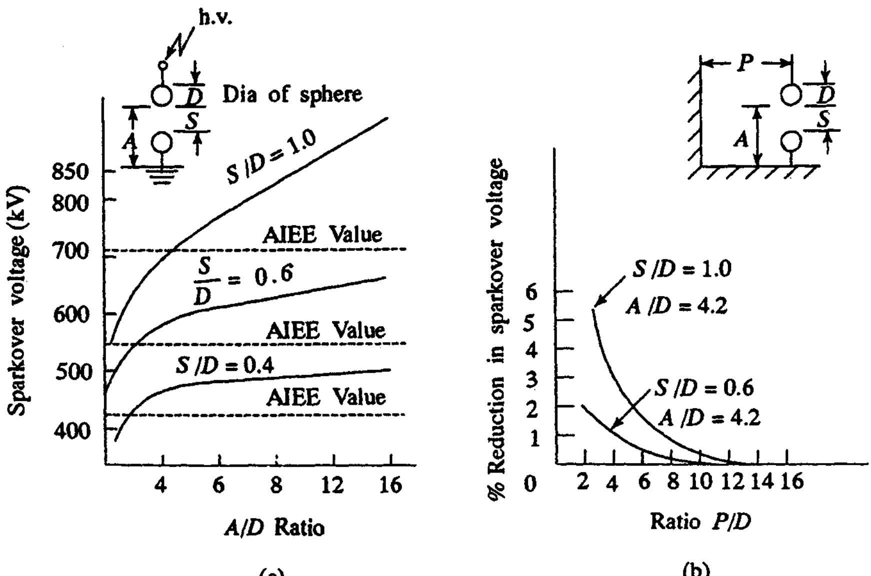

Fig. 7.19 Influence of ground planes on sparkover voltage

(ii) Effect of atmospheric conditions

The sparkover voltage of a spark gap depends on the air density which varies with the changes in both temperature and pressure. If the sparkover voltage is V under test conditions of temperature T and pressure p torr and if the sparkover voltage is V_0 under standard conditions of temperature $T = 20°C$ and pressure $p = 760$ torr, then

$$V = kV_0$$

where k is a function of the air density factor d, given by

$$d = \frac{p}{760}\left(\frac{293}{273+T}\right) \qquad (7.22)$$

The relationship between d and k is given in Table 7.6.

Table 7.6 Relation between Correction Factor k and Air Density Factor d

d	0.70	0.75	0.80	0.85	0.90	0.95	1.0	1.05	1.10	1.15
k	0.72	0.77	0.82	0.86	0.91	0.95	1.0	1.05	1.09	1.12

The sparkover voltage increases with humidity. The increase is about 2 to 3% over normal humidity range of 8 g/m^3 to 15 g/m^3. The influence of humidity on sparkover voltage of a 25 cm sphere gap for 1 cm spacing is presented in Fig. 7.20. It can be seen that the increase in sparkover voltage is less than 3% and the variation between a.c. and d.c. breakdown voltages is negligible (< 0.5%). Hence, it may be concluded that (*i*) the humidity effect increases with the size of spheres and is maximum for uniform field gaps, and (*ii*) the sparkover voltage increases with the partial pressure of water vapour in air, and for a given humidity condition, the change in sparkover voltage

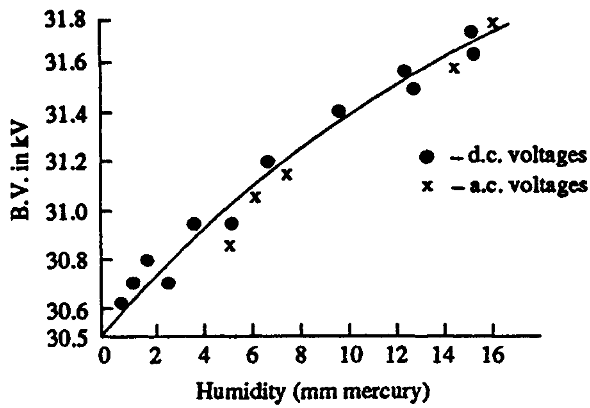

Fig. 7.20 Influence of humidity on d.c. and a.c. breakdown voltages (25 cm dia sphere gap, 1 cm spacing)

increases with the gap length. As the change in sparkover voltage with humidity is within 3%, no correction is normally given for humidity.

(iii) Effect of Irradiation

Illumination of sphere gaps with ultra-violet or x-rays aids easy ionization in gaps. The effect of irradiation is pronounced for small gap spacings. A reduction of about 20% in sparkover voltage was observed for spacings of 0.1 D to 0.3 D for a 1.3 cm sphere gap with d.c. voltages. The reduction in sparkover voltage is less than 5% for gap spacings more than 1 cm, and for gap spacings of 2 cm or more it is about 1.5%. Hence, irradiation is necessary for smaller sphere gaps of gap spacing less than 1 cm for obtaining consistent values.

(iv) Effect of polarity and waveform

It has been observed that the sparkover voltages for positive and negative polarity impulses are different. Experimental investigation showed that for sphere gaps of 6.25 to 25 cm diameter, the difference between positive and negative d.c. voltages is not more than 1%. For smaller sphere gaps (2 cm diameter and less) the difference was about 8% between negative and positive impulses of 1/50 μ s waveform. Similarly, the wave front and wave tail durations also influence the breakdown voltage. For wave fronts of less than 0.5 μ s and wave tails less than 5 μ s the breakdown voltages are not consistent and hence the use of sphere gap is not recommended for voltage measurement in such cases.

Uniform Field Electrode Gaps

Sphere gaps, although widely used for voltage measurements, have only limited range with uniform electric field. Hence, it is not possible to ensure that the sparking always takes place along the uniform field region. Rogowski (see Craggs and Meek[1]) presented a design for uniform field electrodes for sparkover voltages up to 600 kV. The sparkover voltage in a uniform field gap is given by

$$V = AS + B\sqrt{S}$$

where A and B are constants, S is the gap spacing in cm, and V is the sparkover voltage.

Typical uniform field electrodes are shown in Fig. 7.21. The constants A and B were found to be 24.4 and 7.50 respectively at a temperature $T = 25°C$ and pressure = 760 torr. Since the sparking potential is a function of air density, the sparkover voltage for any given air density factor d (see Eq. 7.22) is modified as

$$V = 24.4\, dS + 7.50\sqrt{dS} \tag{7.23}$$

Bruce (see Craggs *et al.*[1] and Kuffel *et al.*[2]) made uniform field electrodes with a sine curve in the end region. According to Bruce, the electrodes with diameters of 4.5, 9.0, and 15.0 in. can be used for maximum voltages of 140, 280, and 420 kV respectively. For the Bruce profile, the constants A and B are respectively 24.22 and 6.08. Later, it was found that with humidity the sparkover voltage increases, and the relationship for sparkover voltage was modified as

$$V = 6.66\sqrt{dS} + [24.55 + 0.41(0.1e - 1.0)]dS \tag{7.24}$$

where, V = sparkover voltage, kV_{peak} (in $kV_{d.c.}$).

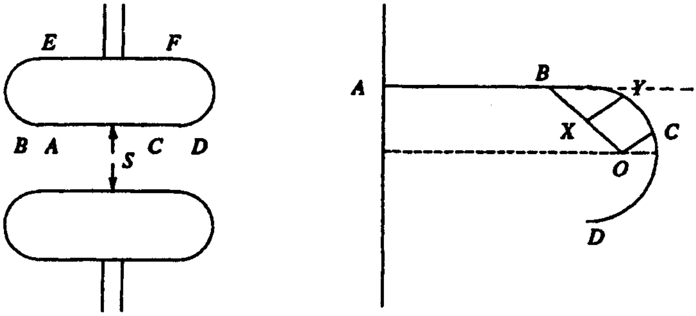

AC, *EF* — Flat portion ($\geq S$)

Curvature *A* to *B* and *C* to $D \geq 108$

Curvature *B* to *E* and *D* to *F* continuously increasing

(a) Electrodes for 300 kV (rms) spark gap

AB — Flat portion
BC — Sine curve
CD — arc of a circle with centre at *O*
XY — $OC \sin\left(\frac{\pi}{2} \cdot \frac{BX}{BO}\right)$

(b) Bruce profile (half contour)

Fig. 7.21 Uniform field electrode spark gap

S = spacing between the electrodes, cm,

d = air density factor, and

e = vapour pressure of water in air (mm Hg).

The constants A and B differ for a.c., d.c., and impulse voltages. A comparison between the sparkover voltages (in air at a temperature of 20°C and a pressure of 760 torr) of a uniform field electrode gap and a sphere gap is given in Table 7.7. From this table it may be concluded that within the specified limitations and error limits, there is no significant difference among the sparkover voltages of sphere gaps and uniform field gaps.

Table 7.7 Sparkover Voltages of Uniform Field Gaps and Sphere Gaps at $t = 20°C$ and $p = 760$ torr

Gap spacing (cm)	Sparkover voltage with uniform field electrodes as measured by			Sphere gap sparkover voltage (kV)
	Ritz (kV)	Bruce (kV)	Schumann (kV)	
0.1	4.54		4.50	4.6
0.2	7.90	7.56	8.00	8.0
0.5	17.00	16.41	17.40	17.0
1.0	31.35	30.30	31.70	31.0
2.0	58.70	57.04	59.60	58.0
4.0	112.00	109.00	114.00	112.0

6.0	163.80	160.20	166.20	164.0
8.0	215.00	211.00	216.80	215.0
10.0	265.00	261.1	266.00	265.0
12.0	315.00	311.6		312.0

The sparkover voltage of uniform field electrode gaps can also be found from calculations. However, no such calculation is available for sphere gaps. In spite of the superior performance and accuracy, the uniform field spark gap is not usually used for measurement purposes, as very accurate finish of the electrode surfaces and careful alignment are difficult to obtain in practice.

Rod Gaps

A rod gap is also sometimes used for approximate measurement of peak values of power frequency voltages and impulse voltages. IEEE recognise that this method gives an accuracy within ±8%. The rods will be either square edged or circular in cross-section. The length of the rods may be 15 to 75 cm and the spacing varies from 2 to 200 cm. The sparkover voltage, as in other gaps, is affected by humidity and air density. The power frequency breakdown voltage for 1.27 cm square rods in air at 25°C and at a pressure of 760 torr with the vapour pressure of water of 15.5 torr is given in Table 7.8. The humidity correction is given in Table 7.9. The air density correction factor can be taken from Table 7.6.

Table 7.8 Sparkover Voltage for Rod Gaps

Gap spacing (cm)	Sparkover voltage (kV)	Gap spacing (cm)	Sparkover voltage (kV)
2	26	30	172
4	47	40	225
6	62	50	278
8	72	60	332
10	81	70	382
15	102	80	435
20	124	90	488
25	147	100	537

The rods are 1.27 cm square edged at t = 27°C, p = 760 torr, and vapour pressure of water = 15.5 torr.

Table 7.9 Humidity Correction for Rod Gap Sparkover Voltages

Vapour pressure of water (torr)	2.54	5	10	15	20	25	30
Correction factor %	– 16.5	– 13.1	– 6.5	– 0.5	4.4	7.9	10.1

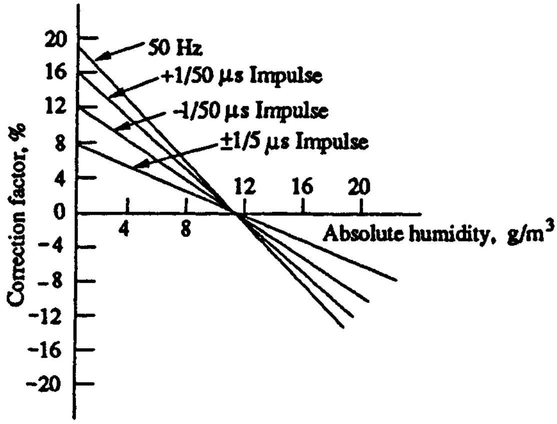

Fig. 7.22 Correction factor for rod gaps

In case of impulse voltage measurements, the IEC and IEEE recommend horizontal mounting of rod gaps on insulators at a height of1.5 to 2.0 times the gap spacing above the ground. One of the rods is usually earthed. For 50% flashover voltages, the procedure followed is the same as that for sphere gaps. Corrections for humidity for 1/50 μ s impulse and 1/50 μ s impulse waves of either polarity are given in Fig. 7.22. The sparkover voltages for impulse waves are given in Table 7.10.

Table 7.10 Sparkover Voltages of Rod Gaps for Impulse Voltages at Temperature = 20°c, Pressure = 760 torr and Humidity = 11 g/cm^2

Gap length (cm)	1/5 μ s wave (kV)		1/50 μ s wave (kV)	
	ositive	Negative	Positive	Negative
5	60	66	56	61
10	101	111	90	97
20	179	208	160	178
30	256	301	226	262
40	348	392	279	339
50	431	475	334	407
60	513	557	397	470
80	657	701	511	585
100	820	855	629	703

7.2.7 Potential Dividers for Impulse Voltage Measurements

Potential or voltage dividers for high voltage impulse measurements, high frequency a.c. measurements, or for fast rising transient voltage measurements are usually either resistive or capacitive or mixed element type. The low voltage arm of the divider is usually connected to a fast recording oscillograph or a peak reading instrument through a delay cable. A schematic diagram of a potential divider with its terminating equipment is given in Fig. 7.23. Z_1 is usually a resistor or a series of resistors in case of a resistance potential divider, or a single or a number of capacitors in case of a capacitance divider. It can also be a combination of both resistors and capacitors. Z_2 will be a resistor or a capacitor or an R-C impedance depending upon the type of the divider. Each element in the divider, in case of high voltage dividers, has a self-resistance or capacitance. In addition, the resistive elements have residual inductances, a terminal stray capacitance to ground, and terminal to terminal capacitances.

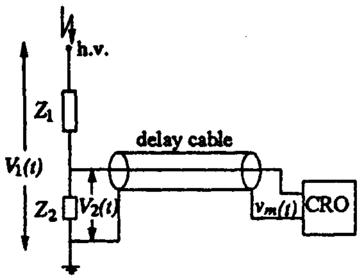

Fig. 7.23 Schematic diagram of a potential divider with a delay cable and oscilloscope

The lumped-circuit equivalent of a resistive element is already shown in Fig. 7.7, and the equivalent circuit of the divider with inductance neglected is of the form shown in Fig. 7.8a. A capacitance potential divider also has the same equivalent circuit as in Fig. 7.7a, where C_s will be the capacitance of each elemental capacitor, C_g will be the terminal capacitance to ground, and R will be the equivalent leakage resistance and resistance due to dielectric loss in the element. When a step or fast rising voltage is applied at the high voltage terminal, the voltage developed across the element Z_2 will not have the true waveform as that of the applied voltage. The cable can also introduce distortion in the waveshape. The following elements mainly constitute the different errors in the measurement:

(*i*) residual inductance in the elements;

(*ii*) stray capacitance occurring

   (*a*) between the elements,

   (*b*) from sections and terminals of the elements to ground, and

   (*c*) from the high voltage lead to the elements or sections;

(*iii*) the impedance errors due to

(*a*) connecting leads between the divider and the test objects, and
(*b*) ground return leads and extraneous current in ground leads; and

(*iv*) parasitic oscillations due to lead and cable inductances and capacitance of high voltage terminal to ground.

The effect to residual and lead inductances becomes pronounced when fast rising impulses of less than one microsecond are to be measured. The residual inductances damp and slow down the fast rising pulses. Secondly, the layout of the test objects, the impulse generator, and the ground leads also require special attention to minimize recording errors. These are discussed in Sec. 7.4.

Resistance Potential Divider for Very Low Impulse Voltages and Fast Rising Pulses

A simple resistance potential divider consists of two resistances R_1 and R_2 in series ($R_1 >> R_2$) (see Fig. 7.24). The attenuation factor of the divider or the voltage ratio is given by

$$a = \frac{V_1(t)}{V_2(t)} = 1 + \frac{R_1}{R_2}. \tag{7.25}$$

The divider element R_2, in practice, is connected through the coaxial cable to the oscilloscope. The cable will generally have a surge impedance Z_0 and this will come in parallel with the oscilloscope input impedance (R_m, C_m). R_m will generally be greater than one megaohm and C_m may be 10 to 50 picofarads. For high frequency and impulse voltages (since they also contain high frequency fundamental and harmonics), the ratio in the frequency domain will be given by

$$a = \frac{V_1}{V_2} = 1 + \frac{R_1}{(R_2/1 + j\omega R_2 C_m)} \tag{7.26}$$

Hence, the ratio is a function of the frequency. To avoid the frequency dependance of the voltage ratio a, the divider is compensated by adding an additional capacitance C_1 across R_1. The value of C_1, to make the divider independent of the frequency, may be obtained from the relation,

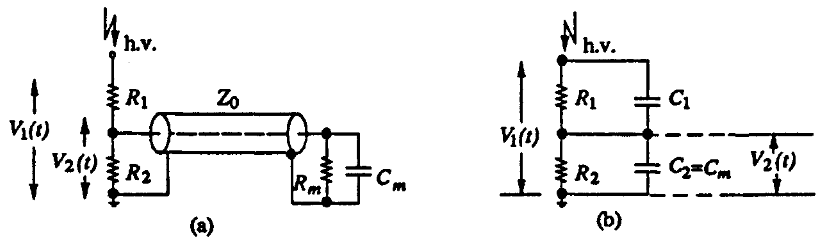

Resistance potential divider with surge cable and oscilloscope terminations

Comepensated resistance potential divider

Fig. 7.24 a & b Resistance potential dividers

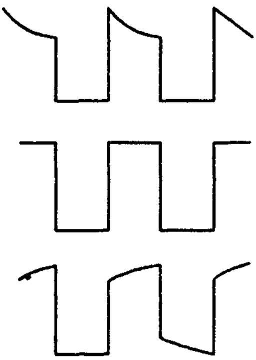

Fig. 7.24c Output of compensated resistance voltage divider for different degrees of compensation

$$\frac{R_1}{R_2} = \frac{C_m}{C_1} \tag{7.27}$$

or, $$R_1 C_1 = R_2 C_m$$

meaning that the time constant of both the arms should be the same. This compensation is used for the construction of high voltage dividers and probes used with oscilloscopes. Usually, probes are made with adjustable values of C_m so that the value of C_m can include any stray capacitance including that of a cable, etc. A typical high voltage probe with a four nanosecond rise time rated for 40 kV (peak) has an input impedance of 100 MΩ in parallel with 2.7 pF. The output waveforms of a compensated divider are shown in Fig. 7.24c with over and under compensation for a square wave input. In Fig. 7.24 c(i) is shown the waveform of an R-C divider when C_1 is too large or overcompensated, while in Fig. 7.24 c(iii) is shown the waveform when C_1 is small or under compensated. For the exponential slope or for the rising portion of the wave, the time constant $\tau = [R_1R_2/(R_1 + R_2)](C_1 + C_m)$. This will be too large when the value of C_1 is greater than that required for correct compensation, i.e. $R_1 C_1 = R_2 C_m$ and hence an overshoot with an exponential decay occurs as shown in Fig. 7.24 c(i). For under compensation, the charging time is too high and as such an exponential rise occurs as shown in Fig. 7.24 c(iii). The schematic circuit of a compensated oscilloscope probe is shown in Fig. 7.25.

Potential Dividers Used for High Voltage Impulse Measurements

In a resistance potential divider, R_1 and R_2 are considered as resistors of small dimensions in the previous section. For voltages above 100 kV, R_1 is no longer small in dimension and is usually made of a number of sections. Hence the divider is no longer a small resistor of lumped parameters, but has to be considered as an equivalent distributed network with its terminal to ground capacitances and inter-sectional series capacitances as shown in Fig. 7.26. The total series resistance R_1 is made of n resistors of value R'_1 and $R = nR'_1$. C_g is the terminal to ground capacitance of each of the

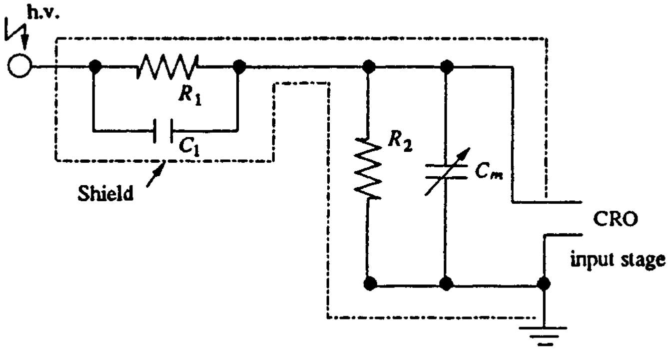

Fig. 7.25 Schematic circuit arrangement of a cathode ray oscilloscope voltage divider probe

resistor elements R'_1, and C_s is the capacitance between the terminals of each section. The inductance of each element (L'_1) is not shown in the figure as it is usually small compared to the other elements (i.e. R'_1, C_s and C_g). This type of divider produces a non-linear voltage distribution along its length and also acts like an R-C filter for applied voltages. The output of such a divider for various values of C_g/C_s ratio is shown in Fig. 7.27 for a step input. By arranging guard rings at various elemental points, the equivalent circuit can be modified as shown in Fig. 7.28, where C_h

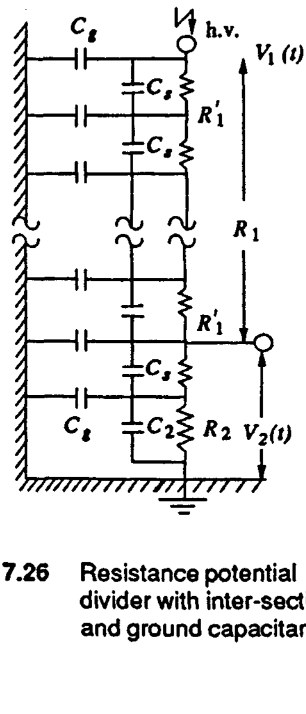

Fig. 7.26 Resistance potential divider with inter-sectional and ground capacitances

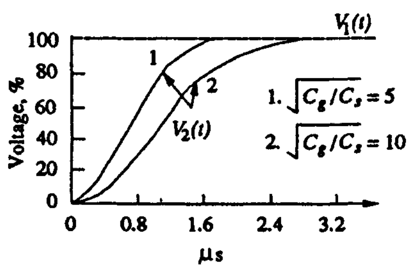

Fig. 7.27 Output of the divider shown in Fig. 7.26 for a step input

represents the stray capacitance introduced between the high voltage lead and the guard elements. This reduces the distortion introduced by the original divider.

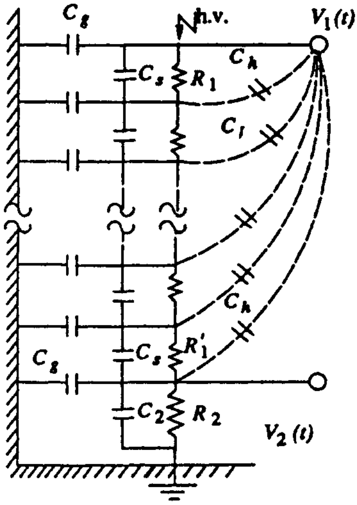

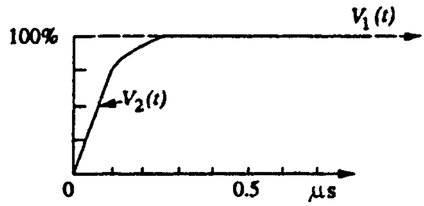

Output of the divider
for a step input voltage

Fig. 7.28 Equivalent circuit of a resistance potential divider with shield and guard rings

Capacitance Voltage Dividers

Capacitance voltage dividers are ideal for measurement of fast rising voltages and pulses. The capacitance ratio is independent of the frequency, if their leakage resistance is high enough to be neglected. But usually the dividers are connected to the source voltage through long leads which introduce lead inductances and residual resistances. Also, the capacitance used for very high voltage work is not small in dimension and hence cannot be considered as a lumped element. Therefore, the output of the divider for high frequencies and impulses is distorted as in the case of resistance dividers.

Pure Capacitance Dividers

A pure capacitance divider for high voltage measurements and its electrical equivalent network without stray elements is shown in Fig. 7.29. The ratio of the divider

$$a = \frac{V_1(t)}{V_2(t)} = 1 + \frac{C_2}{C_1} \tag{7.28}$$

Capacitance C_1 is formed between the h.v. terminal of the source (impulse generator) and that of the test object or any other point of measurement. The CRO is located within the shielded screen surrounding capacitance C_2. C_2 includes the capacitance used, the lead capacitance, input capacitance of the CRO, and other

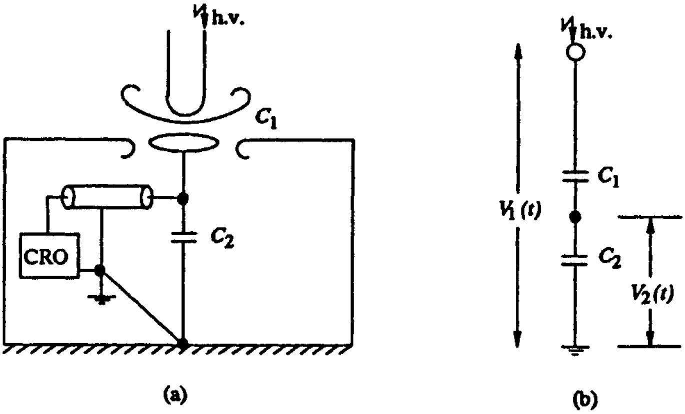

Fig. 7.29 Capacitance voltage divider for very high voltages and its electrical equivalent circuit

ground capacitances. The advantage of this connection is that the loading on the source is negligible; but a small disturbance in the location of C_2 or h.v. electrode or the presence of any stray object nearby changes the capacitance C_1, and hence the divider ratio is affected.

In many cases a standard air or compressed gas capacitor is used which has coaxial cylindrical construction. Accurate ratios that could be calculated up to 1000 : 1 have been achieved for a maximum impulse voltage of 350 kV, and the upper frequency limit is about 10 MHz. For smaller or moderate high voltages (up to 100 kV) capacitance dividers are built with an upper frequency limit of 200 MHz.

Another type of design frequently used is to make C_1 to consist of a number of capacitors C'_1 in series for the given voltage V_1. In such cases the equivalent circuit is similar to that of a string insulator unit used in transmission lines (Fig. 7.30). The voltage distribution along the capacitor chain is non-linear and hence causes distribution of the output wave. But the ratio error is constant and is independent on frequency as compared to resistance dividers. A simplified equivalent circuit is shown in Fig. 7.30 b, which can be used if $C_1 << C_2$ and $C_g << C_1$. The voltage ratio is

$$a = \frac{V_1(t)}{V_2(t)} \approx \left[1 + \frac{C_2}{C_1}\right]\left[1 + \frac{C_g}{6C_1}\right] \qquad (7.29)$$

This ratio is constant and gives an error of less than 5% when $C_1 = 3C_g$. This equivalent circuit is quite satisfactory up to 1 MHz.

Field Controlled Voltage Dividers

The electrostatic or capacitive field distribution of a shield or guard ring placed over a resistive divider to enforce a uniform field in the neighbourhood and along the divider may be adopted for high voltage measurements. The schematic diagram is shown in Fig. 7.31 and its equivalent circuit is same as that given in Fig. 7.28. The shield is of the form of a cone. R_1 is a non-linear resistance in the sense the resistance per unit length is not the same but is variable. The main advantage is that the

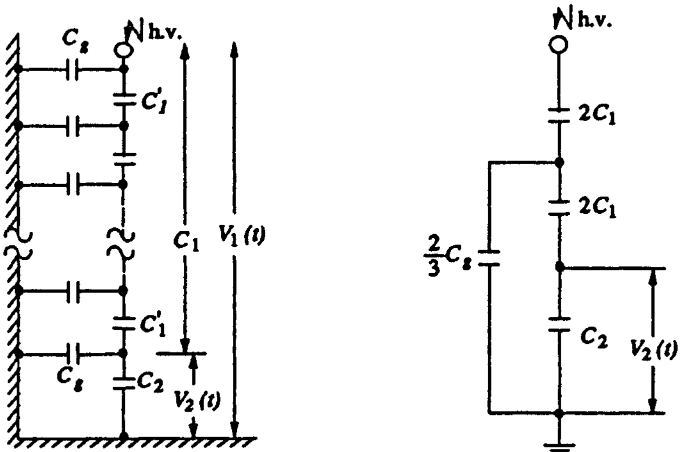

(a) Distributed network

(b) Approximate equivalent circuit

Fig. 7.30 Capacitance voltage divider with distributed network and its equivalent circuit

capacitance per unit length is small and hence loading effect is reduced. Sometimes the parallel resistance R_2 together with the lead inductance and shunt capacitances cause oscillations as shown in Fig. 7.32a. The oscillations can be reduced by adding a damping resistance R_d as shown in Fig. 7.31. Such dividers are constructed for very

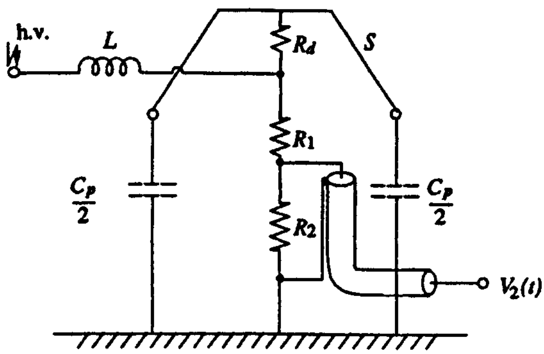

R_d — Damping resistor

L — Lead inductance

C_P — Capacitance of the shield to ground

S— Shield

Fig. 7.31 Field controlled resistance divider with a damping resistor

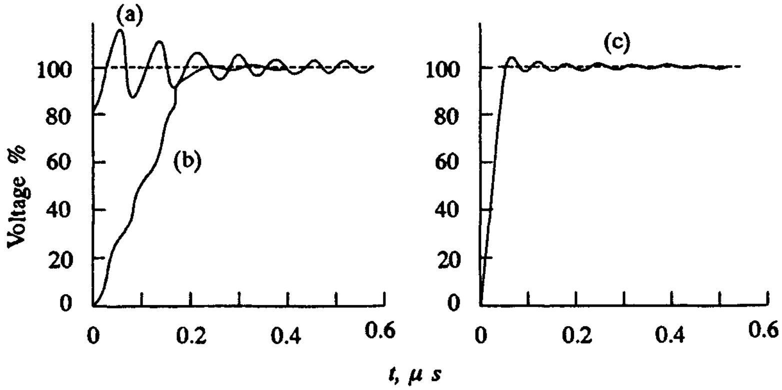

(a) $R_d = 0$ and long lead
(b) $R_d = 0$ and short lead of 14′ long with low inductance
(c) $R_d = 500\ \Omega$ and long lead

Fig. 7.32 Step response of field controlled voltage divider of Fig. 7.31

high voltages (up to 2 MV) with response times less than 30 ns. The resistance column, R_1 is made of woven resistance of 20 kilo ohms. The step response of such a divider is shown in Fig. 7.32, with and without a damping resistor. With a proper damping resistor (R_4) the response time is much less and the overshoot is reduced.

Mixed R-C Potential Dividers

Mixed potential dividers use *R-C* elements in series or in parallel. One method is to connect capacitance in parallel with each R'_1 element. This is successfully employed

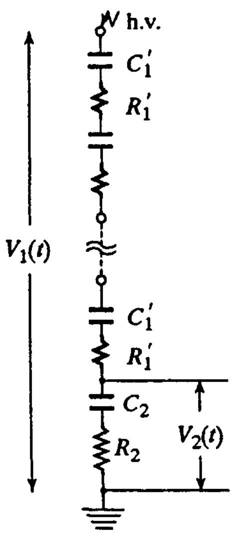

$$R'_1 = \frac{R_1}{n}$$

$$C'_1 = nC_1\left[1 - \frac{C_g}{6\,C_1}\right]$$

C_g = ground capacitance
C_1 = total series capacitance
R_1 = total resistance
$R_1C_1 = R_2C_2$

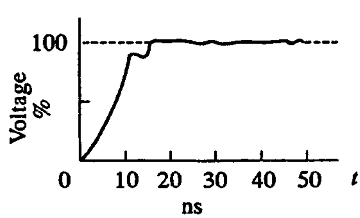

(b) Step response determined with low voltage step pulse

(a) Equivalent circuit

Fig. 7.33 Equivalent circuit of a series R-C voltage divider and its step response for voltage dividers of rating 2 MV and above. A better construction is to make an R-C series element connection. The equivalent circuit of such a construction is shown in Fig. 7.33. Such dividers are made for 5 MV with response times less than 30 n s. The low voltage arm R_2 is given "L peaking" by connecting a variable inductance L in series with R_2. The step response of the divider and the schematic connection of low voltage arm are shown in Fig. 7.34. However, for a correctly designed voltage divider L peaking will not be necessary.

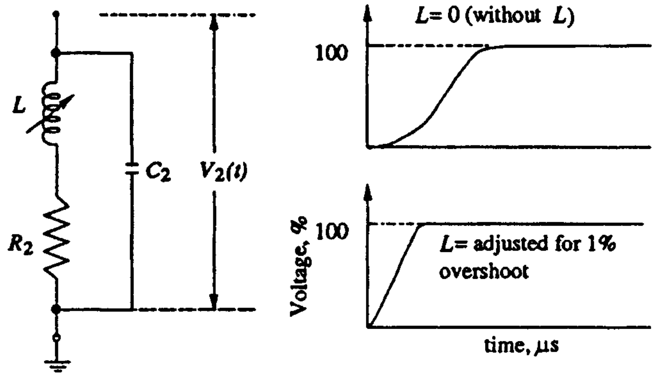

Fig. 7.34 *L* peaking in low voltage arm and step response of the divider with *L* peaking

R-C Potential dividers for 2 MV rating and above

Voltage dividers used for measuring more than one million volts attenuate the measuring signal to a value in the range 100 V to few hundreds of volts. The criteria required to assess the dividers are: (i) the shape of the voltage in the test arrangement should be transferred without any distortion to the L.V. side, (ii) simple determination of transfer behaviour should be ensured, and (iii) they should be suitable for multipurpose use, i.e. for use with a.c. power frequency voltages, switching impulse voltages as well as with lightning impulse voltages. This condition necessitates that the dividers should have broad bandwidths. The above requirements are generally met by (a) optimally damped R-C dividers, or (b) under damped or low damped R-C dividers. The high voltage arm of such dividers consists of series R-C units while the secondary arm is usually an R-C series or parallel circuit. In case of optimally damped dividers, $R_1 = 4\sqrt{L_1/C_g}$, where L_1 is the inductance of the high voltage lead and the H.V. portion of the divider, and C_g is the equivalent capacitance to ground. Usually this resistance will be 400 to 1000 ohms. On the other hand, for low or underdamped dividers, R_1 will be equal to 0.25 to 1.5 times $\sqrt{L/C_1}$ where L is the inductance for the complete measuring loop and C_1 is the capacitance of the H.V. part of the divider. In this case, the normal value of R_1 lies between 50 and 300 ohms. The step response of the two types of dividers mentioned above is shown in Fig. 7.35. In actual practice, because of the large time constant $(R_d + R_1)C_1$, the optimal damped divider affects the voltage shape at the test object. Standard lightning impulses sometimes cannot be generated to the correct standard specifications. As such, R-C potential dividers are

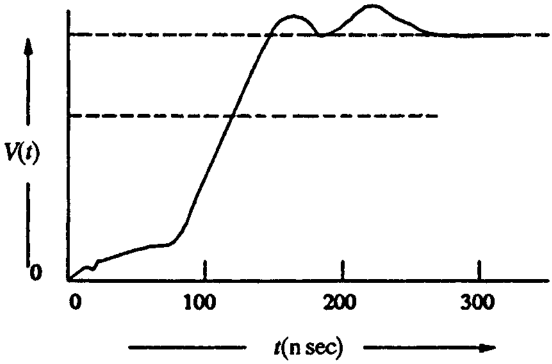

(i) Optimally damped

Response time : 50 n sec
Front time : 50 n sec
Overshoot : $\approx 3\%$
Parameters : $R_1 = 1000\ \Omega$
$C_1 = 360$ pF
Damping resistance : 500 Ω
$(R_d + R_1)\, C_1 = R_2 C_2$

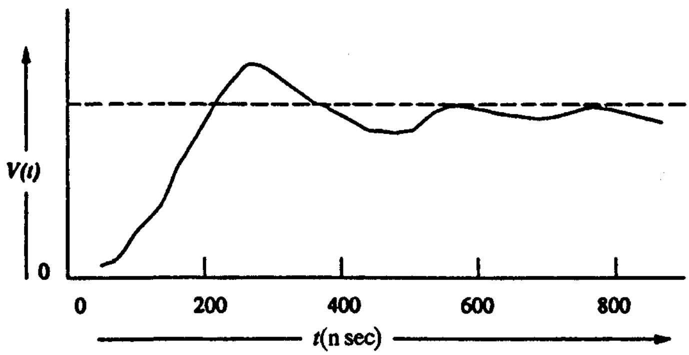

(ii) Underdamped

Response time : 4 n sec
Front time : 110 n sec
Overshoot : $\approx 30\%$
Parameters : $R_1 = 256\ \Omega$
$C_1 = 400$ pF
Damping resistance : 0 Ω
$R_1 C_1 = R_2 C_2$

Fig. 7.35 Step response of a 4 MV R-C divider

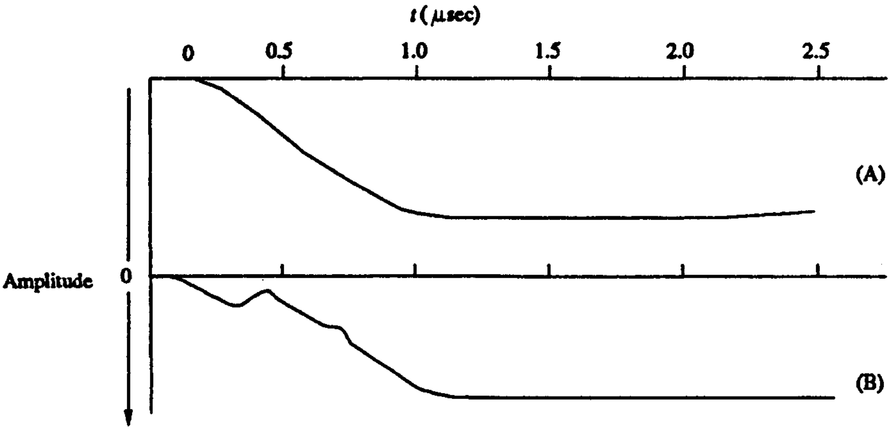

Fig. 7.36 Record of the front portion of a lightning impulse wave with under-damped (curve A) and optimally damped (curve B) dividers for a negative polarity wave when both dividers are connected in parallel

not suitable for measurements with test objects of very low capacitance. The low or underdamped *R-C* divider acts as a load capacitance and a voltage divider, and is suitable for applications over a broad bandwidth, i.e. a.c., switching impulses, lightning impulses, chopped waves etc. Underdamped *R-C* dividers are also suitable for measurement of steep fronted impulse waves. A typical record of lightning impulse wave (1.2/50 μ s wave) obtained using both the above types of dividers is shown in Fig. 7.36. It may be noted that even though the step response is poor in the case of underdamped dividers, they can be used to measure the standard impulse wave to a better accuracy.

Different Connections Employed with Potential Dividers

Different arrangements and connections of voltage or potential dividers with a cathode ray oscilloscope are shown in Figs. 7.37 and 7.38.

A simple arrangement of a resistance divider is shown in Fig. 7.37 a. The possible errors are (*i*) $R_2 \neq Z_0$ (surge impedance of the cable), (*ii*) capacitance of the cable and CRO shunting R_2 and hence introducing distortion, (*iii*) attenuation or voltage drop in surge cable Z_0, and (*iv*) ground capacitance effect. These errors are already discussed in Sec. 7.2.7. To avoid reflections at the junction of the cable and R_2, R_2 is varied and adjusted to give the best possible step response. When a unit function voltage is applied to the circuit shown in Fig. 7.37 b, the effect of the cable is to take a fraction of the voltage $[C_1/(C_1 + C_2)]$ into it and cause reflections at the input end. In the beginning the cable acts like a resistance of value = Z_0 the surge impedance, but later behaves like a capacitor of value equal to the total capacitance of the cable. This behaviour introduces distortion and is compensated by using a split capacitor connection as shown in Fig. 7.37 c with $(C_1 + C_2) = (C_3 + C_k)$ [C_k = capacitance of the cable]. On the other hand if $C_k/(C_1 + C_2 + C_k) = 0.1$, the error will be less than 1.5%.

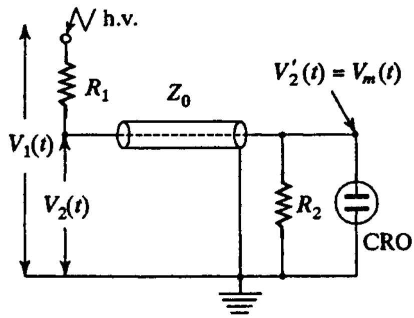

(a) Resistance potential divider with surge cable and CRO

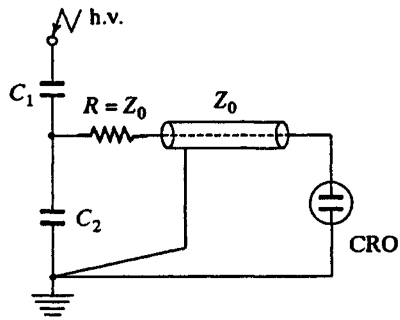

(b) Capacitance divider with surge cable and CRO

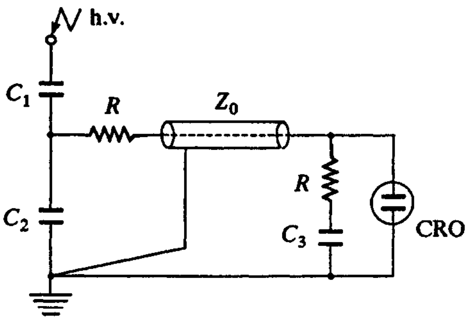

(c) Split capacitor arrangement $R = Z_0$

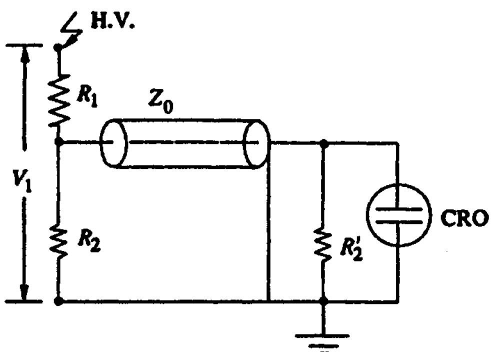

(d) Resistance potential divider with surge cable and CRO.
Voltage ratio, $V_1/V_2 = 1 + (R_1/R_2) + (R_1/R_2')$ where R_2'/Z_0

Fig. 7.37 Potential divider arrangements

The arrangements for mixed potential dividers are shown in Fig. 7.38. The arrangement shown in Fig. 7.38a is modified and improved in the arrangement of Fig. 7.38b. With

$$R_1C_1 = \frac{C_2Z_0(C_1+C_2+C_k)}{(C_1+C_2)} \tag{7.30}$$

$$Z_0 = R_3 + \left(\frac{R_1R_2}{R_1+R_2}\right), \text{ and } R_1C_1 = R_2C_3 \tag{7.31}$$

the response is greatly improved. The arrangement shown in Fig. 7.38c is simple and gives the desired impedance matching.

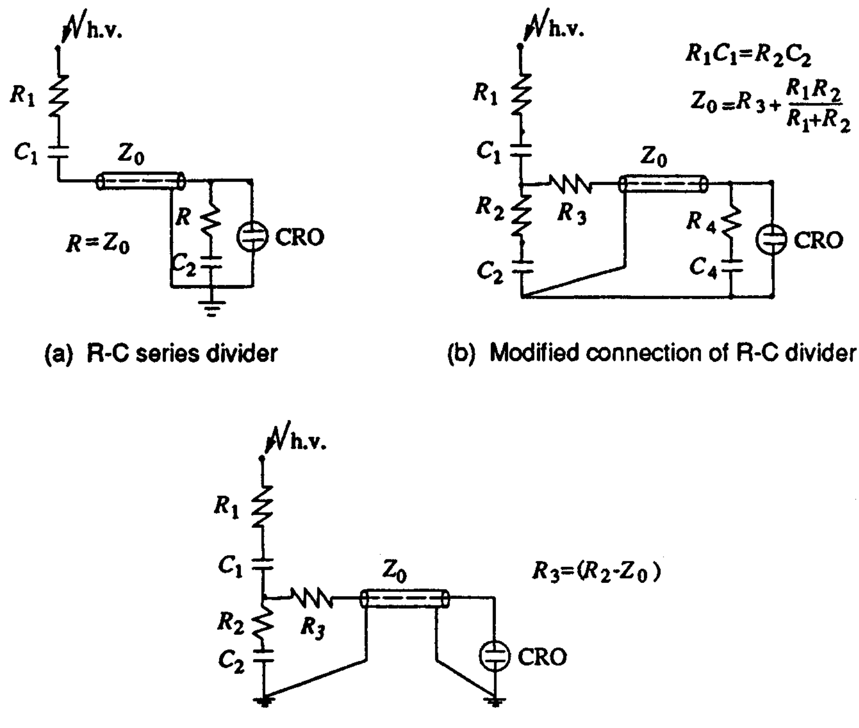

(a) R-C series divider

(b) Modified connection of R-C divider

(c) Impedance matching with R-C divider

Fig. 7.38 Mixed potential divider arrangements

Low voltage arms of the measuring system connected to voltage dividers

The mode of connection and the layout arrangement of the secondary arm of the divider is very critical for the distortionless measurement of fast transients. The L.V. arm of the divider itself introduces large distortions if not properly connected. Different corrections employed for connecting the L.V. arm to the measuring instrument via the signal cables are shown in Figs. 7.37 and 7.38. The signal cable Z_0 may be assumed to be loss-free so that the surge impedance, $Z_0 = \sqrt{L/C}$ is independent of the frequency and the travel time for the signal, $T_0 = \sqrt{LC}$ (refer to Chapter 8 for details). In the case of resistance dividers,.the cable matching is achieved by having a pure resistance, $R_2 = Z_0$ at the end of the cable. The surge cable Z_0 and the resistance R_2 form an integral part of the cable system. Typically, Z_0 has values of 50 or 75 ohms. In actual practice, signal cables do have losses due to skin effect at high frequencies and hence Z_0 becomes a complex quantity. Thus, the matching of R_2 with Z_0 should be done at high frequencies or with a step input as indicated earlier. In the case of long cables, the cable resistance including that of the shield wire should be taken as a part of the matching resistance. The divider ratio in the case of the connection shown in Fig. 7.37 is

$$a = V_1/V_2 = 1 + R_1/R_2 + R_1/R'_2 \text{ and}$$
$$R'_2 = Z_0 \tag{7.32}$$

For the capacitance dividers, the signal cable cannot be completely matched. A low ohmic resistance connected in parallel with C_2 would load the L.V arm and hence, the output gets decreased. Connection of a resistance $R = Z_0$ at the input end (see figures 7.37 and 7.38) will make the voltage across the CRO the same as that across C_2. The transient voltage ratio, at $t = 0$ is given as

$$a = V_1/V_2 = 1 + C_2/C_1 \text{ and}$$
$$\text{effective} = 1 + (C_2 + C_k)/C_1 \text{ for } t >> 2\,T_0 \tag{7.33}$$

Where C_k is the cable capacitance.

Thus, an initial overshoot of $\Delta V = C_k/(C_1 + C_2)$ will appear. This will be either small or negligible for medium and low cable lengths, and for high values of capacitance C_2. This error can be avoided and the response improved in the case of R-C dividers by using the arrangements shown in Fig. 7.38.

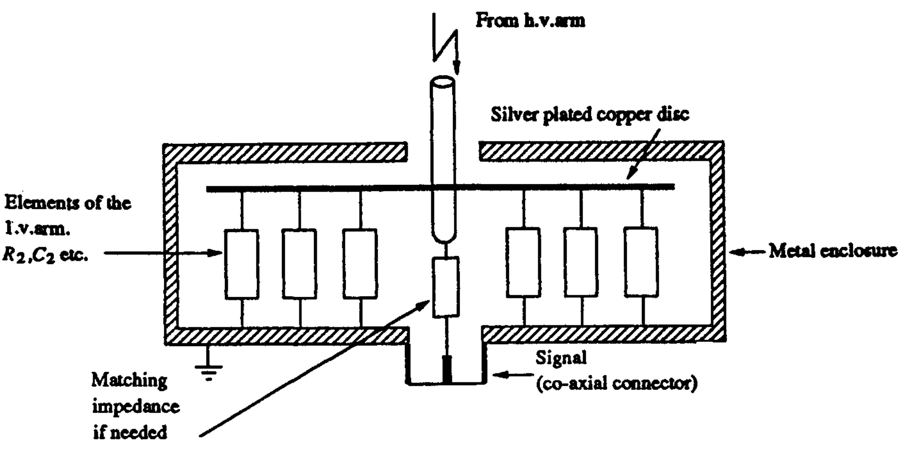

Fig. 7.39 L.V. arm layout for voltage dividers

Usually, the L.V. arms are made co-axial and are enclosed in metal boxes that are solidly grounded. The series resistors used in *R-C* divider forms an integral part of the divider's L.V. arm. Further, all the L.V. arm capacitors and inductors should have a very low inductance. A typical L.V. arm arrangement is shown in Fig. 7.39.

7.2.8 Peak Reading Voltmeters for Impulse Voltages

Sometimes it is enough if the peak value of an impulse voltage wave is measured; its waveshape might already be known or fixed by the source itself. This is highly useful in routine impulse testing work. The methods are similar to those employed for a.c. voltage crest value measurements. The instrument is normally connected to the low voltage arms of the potential dividers described in Sec. 7.2.7. The basic circuit along with its equivalent circuit and the response characteristic is shown in Fig. 7.40. The circuit consists of only valve rectifiers.

Diode D conducts for positive voltages only. For negative pulses, the diode has to be connected in reverse. When a voltage impulse $v(t)$ appears across the low voltage arm of the potential divider, the capacitor C_m is charged to the peak value of the pulse. When the amplitude of the signal starts decreasing the diode becomes reverse biased and prevents the discharging of the capacitor C_m. The voltage developed across C_m is measured by a high impedance voltmeter (an electrostatic voltmeter or an electrometer). As the diode D has finite forward resistance, the voltage to which C_m is charged will be less than the actual peak of the signal, and is modified by the *R-C* network of the diode resistance and the measuring capacitance C_m. The error is shown in Fig. 7.40c. The error can be estimated if the waveform is known. The actual forward

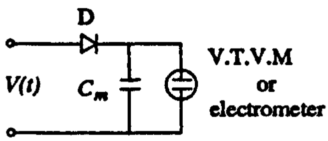

(a) Basic circuit

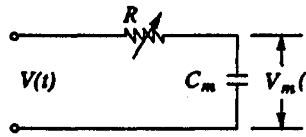

(b) Equivalent circuit of (a) (basic circuit)

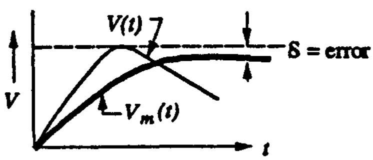

(c) Waveforms of input and meter voltages showing error δ (diode reverse resistance is assumed to be infinite)

Fig. 7.40 A peak reading voltmeter and its equivalent circuit (*R-C* approximation)

 Next Page

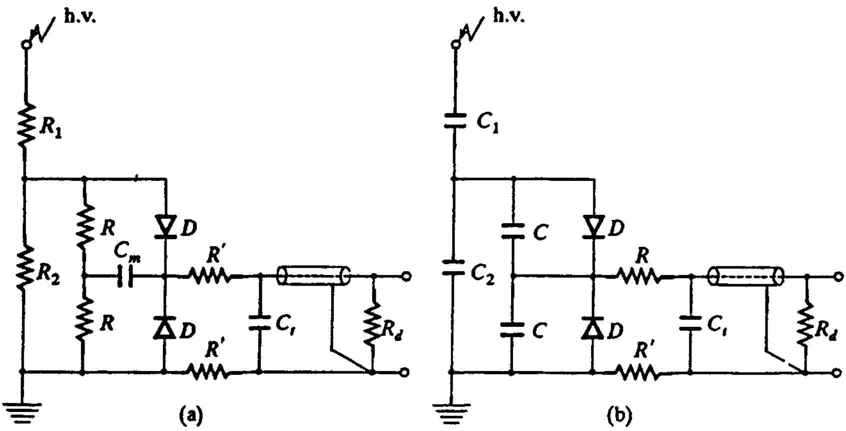

Fig. 7.41 Peak reading voltmeter for either polarity with (a) resistance divider, and (b) capacitance divider

resistance of the diode D (dynamic value) is difficult to estimate, and hence the meter is calibrated using an oscilloscope. Peak voltmeters for either polarity employing resistance dividers and capacitance dividers are shown in Fig. 7.41. In this arrangement, the voltage of either polarity is transferred into a proportional positive measuring signal by a resistive or capacitive voltage divider and a diode circuit. An active network with feedback circuit is employed in commercial instruments, so that the fast rising pulses can also be measured. Instruments employing capacitor dividers require discharge resistance across the low voltage arm to prevent the build-up of d.c. charge.

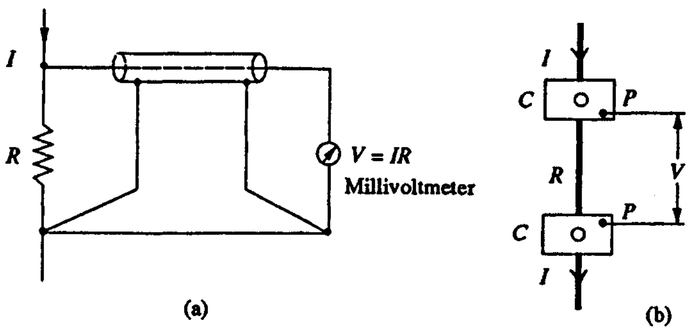

Low ohmic shunt with a millivoltmeter for current measurement

Four terminal shunt

CC — Current terminals
PP — Potential terminals
R — Ohmic element

(In 3 terminal construction the bottom *C* and *P* terminals are made common)

Fig. 7.42 Calibrated ohmic shunt for d.c. current measurements

Previous Page

7.3 MEASUREMENT OF HIGH d.c., a.c. AND IMPULSE CURRENTS

In power systems, it is often necessary to measure high currents, arising due to short circuits. For conducting temperature rise and heat run tests on power equipments like conductors, cables, circuit breakers, etc., measurement of high currents is required. During lightning discharges and switching transients also, large magnitudes of impulse and switching surge currents occur, which require special measuring techniques at high potential levels.

7.3.1 Measurement of High Direct Currents

High magnitude direct currents are measured using a resistive shunt of low ohmic value. The voltage drop across the resistance is measured with a millivoltmeter. The value of the resistance varies usually between 10 μΩ and 13 mΩ. This depends on the heating effect and the loading permitted in the circuit. High current resistors are usually oil immersed and are made as three or four terminal resistances (see Fig. 7.42). The voltage drop across the shunt is limited to a few millivolts (< 1 Volt) in power circuits.

Hall Generators for d.c. Current Measurements

The principle of the "Hall effect" is made use of in measuring very high direct currents. If an electric current flows through a metal plate located in a magnetic field perpendicular to it, Lorenz forces will deflect the electrons in the metal structure in a direction normal to the direction of both the current and the magnetic field. The charge displacement generates an emf in the normal direction, called the "Hall voltage". The Hall voltage is proportional to the current i, the magnetic flux density B, and the reciprocal of the plate thickness d; the proportionality constant R is called the "Hall coefficient".

$$V_H = R\frac{B_i}{d} \tag{7.34}$$

For metals the Hall coefficient is very small, and hence semi-conductor materials are used for which the Hall coefficient is high.

In large current measurements, the current carrying conductor is surrounded by an iron cored magnetic circuit, so that the magnetic field intensity $H = (I/\delta)$ is produced in a small air gap in the core. The Hall element is placed in the air gap (of thickness δ), and a small constant d.c. current is passed through the element. The schematic arrangement is shown in Fig. 7.43. The voltage developed across the Hall element in the normal direction is proportional to the d.c. current I. It may be noted that the Hall coefficient R depends on the temperature and the high magnetic field strengths, and suitable compensation has to be provided when used for measurement of very high currents.

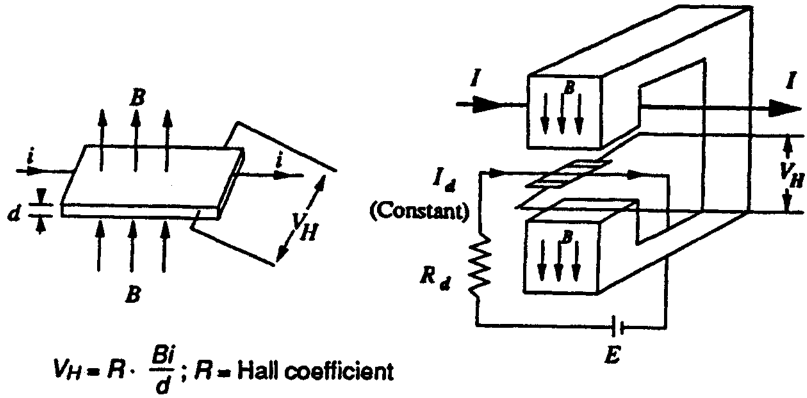

(a) Hall effect (b) Hall generator

Fig. 7.43 Hall generator for measuring high d.c. currents

7.3.2 Measurement of High Power Frequency Alternating Currents

Measurement of power frequency currents are normally done using current transformers only, as use of current shunts involves unnecessary power loss. Also the current transformers provide electrical isolation from high voltage circuits in power systems. Current transformers used for extra high voltage (EHV) systems are quite different from the conventional designs as they have to be kept at very high voltages from the ground. A new scheme of current transformer measurements introducing

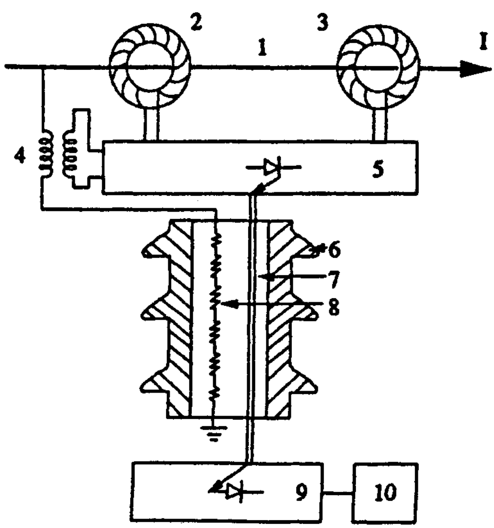

1. EHV conductor
2. Current sensing transformer
3. Power supply C.T.
4. Power supply P.T.
5. Analog-digital signal converter
6. Insulator for EHV
7. Electro-optical glass fibre
8. Series high ohmic resistance
9. Digital-analog converter
10. Indicating or recording unit

Fig. 7.44 Current transformer with electro-optical signal converter for EHV systems electro-optical technique is described in Fig. 7.44. A voltage signal proportional to the measuring current is generated and is transmitted to the ground side through an electro-optical device. Light pulses proportional to the voltage signal are transmitted by a glass-optical fibre bundle to a photodetector and converted back into an analog voltage signal. Aceuracies better than ±0.5% have been obtained at rated current as well as for high short circuit currents. The required power for the signal converter and optical device are obtained from suitable current and voltage transformers as shown in the Fig. 7.44.

7.3.3 Measurement of High Frequency and Impulse Currents

In power system applications as well as in other scientific and technical fields, it is often necessary to determine the amplitude and waveforms of rapidly varying high currents. High impulse currents occur in lightning discharges, electrical arcs and post arc phenomenon studies with circuit breakers, and with electric discharge studies in plasma physics. The current amplitudes may range from a few amperes to few hundred kiloamperes. The rate of rise for such currents can be as high as 10^6 to 10^{12} A/s, and rise times can vary from few microseconds to few nano seconds. In all such cases the sensing device should be capable of measuring the signal over a wide frequency band. The methods that are frequently employed are (*i*) resistive shunts, (*ii*) magnetic potentiometers or probes, and (*iii*) the Faraday and Hall effect devices.

The accuracy of measurement varies from 1 to 10%. In applications where only peak value measurement is required, peak reading voltmeters described in Sec. 7.2.8 may be employed with a suitable shunt.

Resistive shunts

The most common method employed for high impulse current measurements is a low ohmic pure resistive shunt shown in Fig. 7.45. The equivalent circuit is shown in Fig. 7.45b. The current through the resistive element R produces a voltage drop $v(t) = i(t)R$. The voltage signal generated is transmitted to a CRO through a coaxial cable of surge impedance Z_0. The cable at the oscilloscope end is terminated by a resistance $R_i = Z_0$

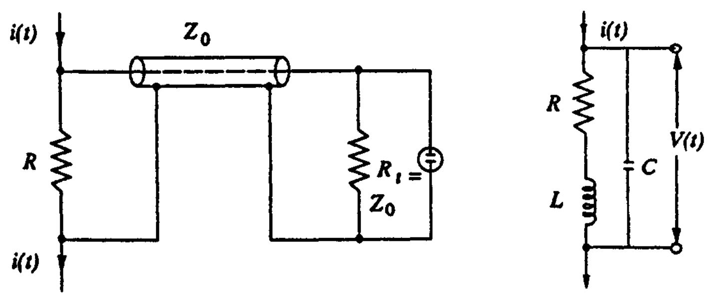

(a) Ohmic shunt (b) Equivalent circuit of the shunt

Fig. 7.45 Calibrated low ohmic shunt and its equivalent circuit for impulse current measurements to avoid reflections. The resistance element, because of its large dimensions will have a residual inductance L and a terminal capacitance C. The inductance L may be neglected at low frequencies (ω), but becomes appreciable at higher frequencies (ω) when ωL is of the order of R. Similarly, the value of C has to be considered when the reactance $1/\omega C$ is of comparable value. Normally L and C become significant above a frequency of 1 MHz. The resistance value usually ranges from 10 $\mu\Omega$ to few milliohms, and the voltage drop is usually about a few volts. The value of the resistance is determined by the thermal capacity and heat dissipation of the shunt.

The voltage drop across the shunt in the complex frequency domain may be written as:

$$V(s) = \frac{(R + Ls)}{(1 + RCs + LCs^2)} I(s) \tag{7.35}$$

where s is the complex frequency or Laplace transform operator and $V(s)$ and $I(s)$ are the transformed quantities of the signals $v(t)$ and $i(t)$. With the value of C neglected it may be approximated as:

$$V(s) = (R + Ls)I(s) \tag{7.36}$$

It may be noted here that the stray inductance and capacitance should be made as small as possible for better frequency response of the shunt. The resistance shunt is usually designed in the following manner to reduce the stray effects.

(*a*) Bifilar flat strip design,
(*b*) coaxial tube or Park's shunt design, and
(*c*) coaxial squirrel cage design

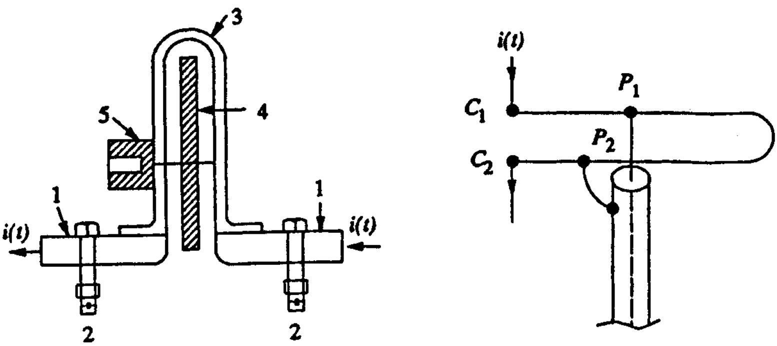

(a) Schematic arrangement

(b) Connection for potential and current terminals

1. Metal base
2. Current terminals (C_1 and C_2)
3. Bifilar resistance strip
4. Insulating spacer (teflon or bakelite)
5. Coaxial UHF connector

P_1, P_2 — Potential terminals

Fig. 7.46 Bifilar flat strip resistive shunt

(a) Bifilar Strip Shunt

The bifilar design (Fig. 7.46) consists of resistor elements wound in opposite directions and folded back, with both ends insulated by a teflon or other high quality insulation. The voltage signal is picked up through a ultra high frequency (UHF) coaxial connector. The shunt suffers from stray inductance associated with the resistance element, and its potential leads are linked to a small part of the magnetic flux generated by the current that is measured. To overcome these problems, coaxial shunts are chosen.

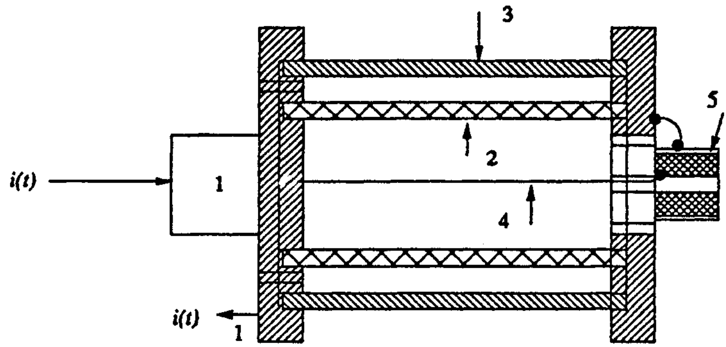

1. Current terminals
2. Coaxial cylindrical resistive element
3. Coaxial cylindrical return conductor (copper or brass tube)
4. Potential pick up lead
5. UHF coaxial connector

Fig. 7.47 Schematic arrangement of a coaxial ohmic shunt

(b) Coaxial Tubular or Park's Shunt

In the coaxial design (Fig. 7.47) the current is made to enter through an inner cylinder or resistive element and is made to return through an outer conducting cylinder of copper or brass. The voltage drop across the resistive element is measured between the potential pick-up point and the outer case. The space between the inner and the outer cylinder is air and hence acts like a pure insulator. With this construction, the maximum frequency limit is about 1000 MHz and the response time is a few nanoseconds. The upper frequency limit is governed by the skin effect in the resistive element. The equivalent circuit of the shunt is given in Fig. 7.48. The step response and the frequency response are shown in Fig. 7.49. The inductance L_0 shown in Fig. 7.48 may be written as:

$$L_0 = \frac{\mu d l}{2\pi r} \tag{7.37}$$

where, $\mu = \mu_0 \mu_r$; the magnetic permeability, $\mu_0 = 4\pi \times 10^{-9}$ Vs/A cm is the magnetic field constant of vacuum

$d =$ thickness of the cylindrical tube,

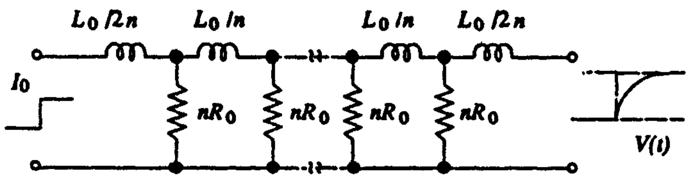

(a) Exact equivalent circuit

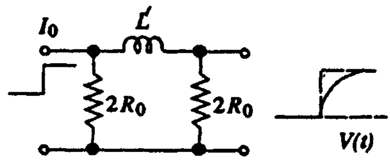

(b) Simplified circuit

L_0 — Inductance
R_0 — d.c. resistance
n — Number of sections per unit length

L' — 0.43 L_0

Fig. 7.48 Simplified and exact equivalent circuits of a coaxial tubular shunt

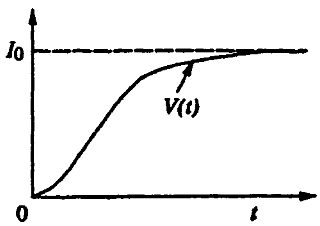

(a) Step response

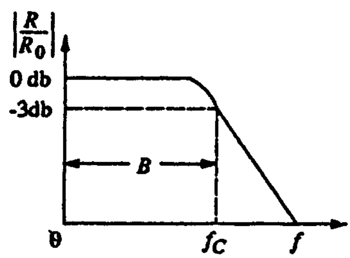

B = Band width
f_C = Maximum frequency limit.

(b) Frequency response

Fig. 7.49 Step and frequency responses of a coaxial tubular shunt

l = length of the cylindrical tube, and
r = radius of the cylindrical tube

The effective resistance is given by

$$R = \frac{V(t)}{I_0} = R_0\theta(\omega t) \tag{7.38}$$

where, R_0 = the d.c. resistance; L_0 = inductance for d.c. currents and $\theta(\omega t)$ is the theta function of type 3 and is equal to

$$[1 + 2 \sum_{n=1}^{\infty} (-1)^n \exp(-n^2 \omega t)]$$

in which $\omega = \dfrac{(\pi^2 R_0)}{L_0}$

$V(t)$ = signal developed; and I_0 is the step current.

The effective impedance of the shunt for any frequency f according to Silsbee is given by:

$$Z = \frac{R_0(1+j)\delta}{\sinh[(1+j)\delta]} \tag{7.39}$$

where,
R_0 = d.c. resistance Ω,
$\delta = 2\pi d\sqrt{(f\mu)/\rho}$,
ρ = resistivity of the material, Ω-cm,
d = thickness of the tube, cm,
f = frequency, Hz, and
μ = permeability as defined earlier.

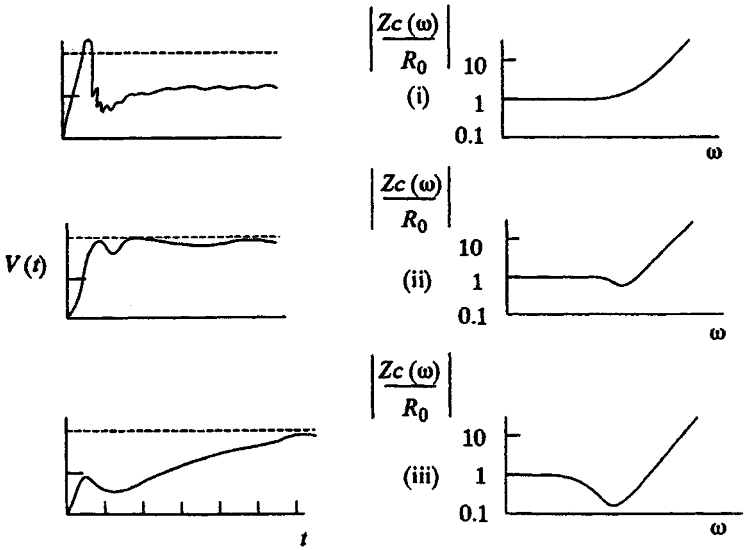

(a) Step response (b) Frequency response

(i) number of rods too small
(ii) ideal number of rods
(iii) number of rods too high

Fig. 7.50 Response of squirrel cage shunt for different number of rods

The simplified equivalent circuit shown in Fig. 7.48 is convenient to calculate the rise time of the shunt. The rise time accordingly is given by,

$$T = 0.237\frac{\mu d^2}{\rho}$$

and the bandwidth is given by

$$B = \frac{1.46R}{L_0} = \frac{1.46\rho}{\mu d^2} \tag{7.40}$$

The coaxial tubular shunts were constructed for current peaks up to 500 kA; shunts constructed for current peaks as high as 200 kA with di/dt of about 5×10^{10} A/s have induced voltages less than 50 V and the voltage drop across the shunt was about 100 V.

(c) Squirrel Cage Shunts

In certain applications, such as post arc current measurements, high ohmic value shunts which can dissipate larger energy are required. In such cases tubular shunts are not suitable due to their limitations of heat dissipation, larger wall thickness, and the skin effect. To overcome these problems, the resistive cylinder is replaced by thick rods or strips, and the structure resembles the rotor construction of double squirrel cage induction motor. The equivalent circuit for squirrel cage construction is different, and complex. The shunts show peaky response for step input, and a compensating network has to be designed to get optimum response. In Fig. 7.50, the step response (Fig. 7.50a) and frequency response (Fig. 7.50b) characteristics are given. Rise times of better than 8 n s with bandwidth more than 400 MHz were obtained for this type of shunts. A typical R-C compensating network used for these shunts is shown in Fig. 7.51.

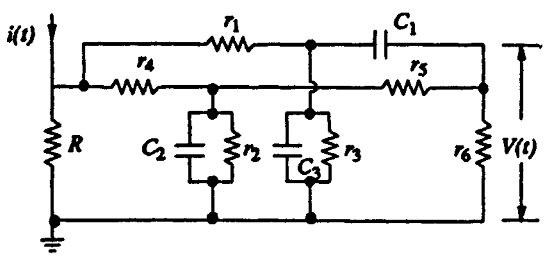

R — Shunt resistance
$r_1 - r_6$ — Resistors and capacitors in compensating double T network and $C_1 - C_6$

Fig. 7.51 Compensating network for squirrel cage shunts

(d) Materials and Technical Data for the Current Shunts

The important factor for the materials of the shunts is the variation of the resistivity of the material with temperature. In Table 7.11 physical properties of some materials with low temperature coefficient, which can be used for shunt construction are given.

Table 7.11 Properties of Resistive Materials

Property	Material				
	Constantan	Manganin	Nichrome	German silver	Ferro-alloy
Resistivity ρ at 20°C (Ω-m)	0.49×10^{-6}	0.43×10^{-6}	1.33×10^{-6}	0.23×10^{-6}	0.49×10^{-6}
Temperature coefficient per °C(10^{-6})	30	20	20	$\approx$ 50	40
Density at 20°C kg/litre	8.9	8.4	8.1	$\approx$ 7.5	8.8
Specific heat kilo calories/ kg °C	0.098	0.097	0.11	$\approx$ 0.1	$\approx$ 0.1

The importance of the skin effect has been pointed out in the coaxial shunt design. The skin depth d for a material of conductivity σ at any frequency f is given by

$$d = \frac{1}{\sqrt{\pi f \mu \sigma}} \tag{7.41}$$

Skin depth, d, is defined as the distance or depth from the surface at which the magnetic field intensity is reduced to '$1/e$' ($e = 2.718\ldots$) of the surface value for a given frequency f. Materials of low conductivity σ (high resistivity materials) have large skin depth and hence exhibit less skin effect.

It may be stated that low ohmic shunts of coaxial type or squirrel cage type construction permit measurements of high currents with response times less than 10 n s.

Measurement of High Impulse Currents Using Magnetic Potentiometers (Rogowski Coils) and Magnetic Links

If a coil is placed surrounding a current carrying conductor, the voltage signal induced in the coil is $v_i(t) = M dI(t)/dt$ where M is the mutual inductance between the conductor and the coil, and $I(t)$ is the current flowing in the conductor. Usually, the coil is wound on a nonmagnetic former of toroidal shape and is coaxially placed surrounding the current carrying conductor. The number of turns on the coil is chosen to be large, to get enough signal induced. The coil is wound cross-wise to reduce the leakage inductance. Usually an integrating circuit (see Fig. 7.52) is employed to get the output signal voltage proportional to the current to be measured. The output voltage is given by

$$V_m(t) = \frac{1}{CR}\int_0^t v_i(t) = \frac{M}{CR} I(t) \tag{7.42}$$

Rogowski coils with electronic or active integrator circuits have large bandwidths (about 100 MHz). At frequencies greater than 100 MHz the response is affected by

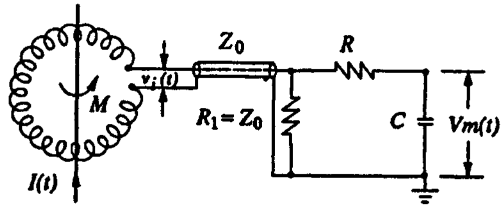

$V_i(t)$ — Induced voltage in the coil $= M\dfrac{d[I(t)]}{dt}$

Z_0 — Coaxial cable of surge impedance Z_0

R-C — Integrating network

Fig. 7.52 Rogowski coil for high impulse current measurements

the skin effect, the capacitance distributed per unit length along the coil, and due to the electromagnetic interferences. However, miniature probes having nanosecond response time are made using very few turns of copper strips for UHF measurements.

Magnetic Links

Magnetic links are short high retentivity steel strips arranged on a circular wheel or drum. These strips have the property that the remanent magnetism for a current pulse of 0.5/5 μ s is same as that caused by a d.c. current of the same value. Hence, these can be used for measurement of peak value of impulse currents. The strips will be kept at a known distance from the current carrying conductor and parallel to it. The remanent magnetism is then measured in the laboratory from which the peak value of the current can be estimated. These are useful for field measurements, mainly for estimating the lightning currents on the transmission lines and towers. By using a number of links, accurate measurement of the peak value, polarity, and the percentage oscillations in lightning currents can be made.

Other Techniques for Impulse Current Measurements

(*a*) *Hall Generators*

Hall generators described earlier can be used for a.c. and impulse current measurements also. The bandwidth of such devices was found to be about 50 MHz with suitable compensating devices and feedback. The saturation effect in magnetic core can be minimized, and these devices are successfully used for post arc and plasma current measurements.

(*b*) *Faraday Generator or Ammeter*

When a linearly polarized light beam passes through a transparent crystal in the presence of a magnetic field, the plane of polarization of the light beam undergoes rotation.

The angle of rotation α is given by:

$$\alpha = VBl \tag{7.43}$$

where, $V =$ a constant of the crystal which depends on the wavelength of the light,

$B =$ magnetic flux density, and

$l =$ length of the crystal.

To measure the waveform of a large current in a EHV system an arrangement shown in Fig. 7.53 may be employed. A beam of light from a stabilized light source is passed through a polarizer P_1 to fall on a crystal F placed parallel to the magnetic field produced by the current I. The light beam undergoes rotation of its plane of polarization. After passing through the analyser, the beam is focused on a photo-multiplier, the output of which is fed to a CRO. The output beam is filtered through a filter M, which allows only the monochromatic light. The relation between the oscillograph display and the current to be measured are complex but can be determined. The advantages of this method are that (*i*) there is no electric connection between the source and the device, (*ii*) no thermal problems even for large currents of several kiloamperes, and (*iii*) as the signal transmission is through an optical system, no insulation problems or difficulties arise for EHV systems. However, this device does not operate for d.c. currents.

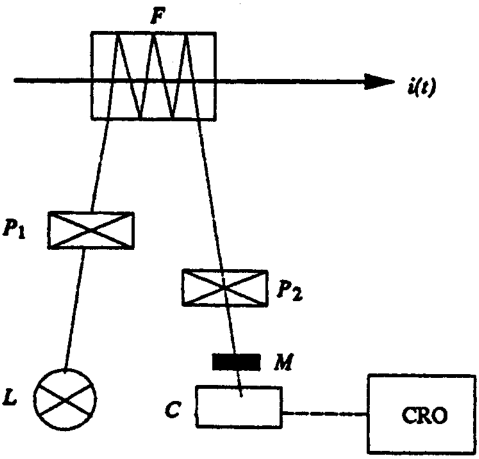

L — Light source
P_1 — Polarizer
P_2 — Analyser
F — Crystal
CRO — Recording oscillograph
M — Filter
C — Photo-multiplier

Fig. 7.53 Magneto-optical method of measuring impulse currents

7.4 CATHODE RAY OSCILLOGRAPHS FOR IMPULSE VOLTAGE AND CURRENT MEASUREMENTS

When waveforms of rapidly varying signals (voltages or currents) have to be measured or recorded, certain difficulties arise. The peak values of the signals in high voltage measurements are too large, may be several kilovolts or kiloamperes. Therefore, direct measurement is not possible. The magnitudes of these signals are scaled down by voltage dividers or shunts to smaller voltage signals. The reduced signal $V_m(t)$ is normally proportional to the measured quantity. The procedure of transmitting the signal and displaying or recording it is very important. The associated electromagnetic fields with rapidly changing signals induce disturbing voltages, which have to be avoided. The problems associated in the above procedure are discussed in this section.

7.4.1 Cathode Ray Oscillographs for Impulse Measurements

Modern oscillographs are sealed tube hot cathode oscilloscopes with photographic arrangement for recording the waveforms. The cathode ray oscilloscope for impulse work normally has input voltage range from 5 mV/cm to about 20 V/cm. In addition, there are probes and attenuators to handle signals up to 600 V (peak to peak). The bandwidth and rise time of the oscilloscope should be adequate. Rise times of 5 n s and bandwidth as high as 500 MHz may be necessary.

Sometimes high voltage surge test oscilloscopes do not have vertical amplifier and directly require an input voltage of 10 V. They can take a maximum signal of about 100 V (peak to peak) but require suitable attenuators for large signals.

Oscilloscopes are fitted with good cameras for recording purposes. Tektronix model 7094 is fitted with a lens of 1 : 1.2 polaroid camera which uses 10,000 ASA film which possesses a writing speed of 9 cm/n s.

With rapidly changing signals, it is necessary to initiate or start the oscilloscope time base before the signal reaches the oscilloscope deflecting plates, otherwise a portion of the signal may be missed. Such measurements require an accurate initiation of the horizontal time base and is known as triggering. Oscilloscopes are normally provided with both internal and external triggering facility. When external triggering is used, as with recording of impulses, the signal is directly fed to actuate the time

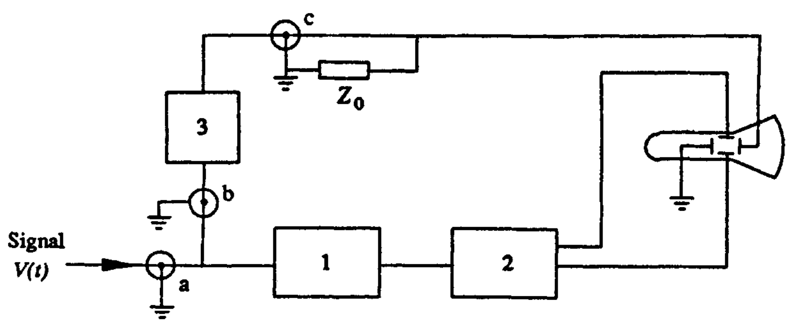

1. Trigger amplifier
2. Sweep generator
3. External delay line

(a) Vertical amplifier input
(b) Input to delay line
(c) Output of delay line to CRO *Y* plates

Fig. 7.54a Block diagram of a surge test oscilloscope (older arrangement)

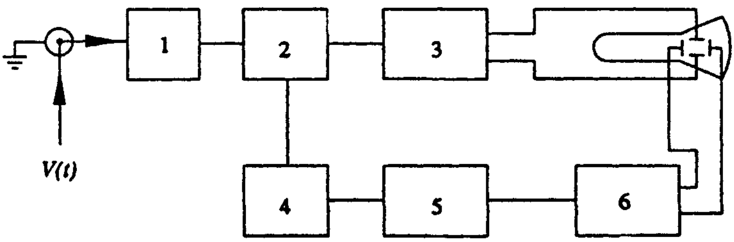

1. Plug-in amplifier
2. Y amplifier
3. Internal delay line
4. Trigger amplifier
5. Sweep generator
6. X amplifier

Fig. 7.54b Simplified block diagram of surge test oscilloscopes (recent schemes)

base and then applied to the vertical or Y deflecting plates through a delay line. The delay is usually 0.1 to 0.5 μ s. The delay is obtained by:

(1) A long interconnecting coaxial cable 20 to 50 m long. The required triggering is obtained from an antenna whose induced voltage is applied to the external trigger terminal.
(2) The measuring signal is transmitted to the CRO by a normal coaxial cable. The delay is obtained by an externally connected coaxial long cable to give the necessary delay. This arrangement is shown in Fig. 7.54.
(3) The impulse generator and the time base of the CRO are triggered from an electronic tripping device. A first pulse from the device starts the CRO time base and after a predetermined time a second pulse triggers the impulse generator.

7.4.2 Instrument Leads and Arrangement of Test Circuits

It is essential that leads, layout, and connections from the signal sources to the CRO are to be arranged such that the induced voltages and stray pick-ups due to electromagnetic interference are avoided. For slowly varying signals, the connecting cables behave as either capacitive or inductive depending on the load at the end of the cable. For fast rising signals, however, the cables have to be accounted as transmission lines with distributed parameters. A travelling wave or signal entering such a cable encounters the surge impedance of the cable. To avoid unnecessary reflections at the cable ends, it has to be terminated properly by connecting a resistance equal to the surge impedance of the cable. In cables, the signal travels with a velocity less than that of light which is given by:

$$v = \frac{C}{\sqrt{\varepsilon_r \mu_r}}$$

where $C = 3 \times 10^8$ m/s and ε_r and μ_r are the relative permittivity and relative permeability respectively of the cable materials. Therefore the cable introduces a finite propagation time

$$t = \frac{1}{v} \times \text{length of the cable}$$

Measuring devices such as oscilloscopes have finite input impedance, usually about 1 to 10 MΩ resistance in parallel with a 10 to 50 pF capacitance. This impedance at high frequencies ($f \approx 100$ MHz) is about 80Ω and thus acts as a load at the end of a surge cable. This load attenuates the signal at the CRO end.

Cables at high frequencies are not lossless transmission lines. Because of the ohmic resistance loss in the conductor and the dielectric loss in the cable material, they introduce attenuation and distortion to the signal. Cable distortion has to be eliminated as far as possible. Cable shields also generate noise, voltages due to ground loop currents and due to the electromagnetic coupling from other conductors. In Fig. 7.55, the ground loop currents and their path are indicated. To eliminate these noise voltages multiple shielding arrangement as shown in Fig. 7.56 may have to be used.

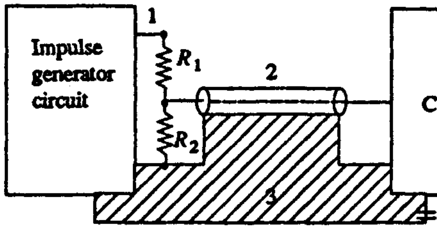

1. Potential divider
2. Coaxial signal cable
3. Ground loop

Fig. 7.55 Ground loops in impulse measuring systems

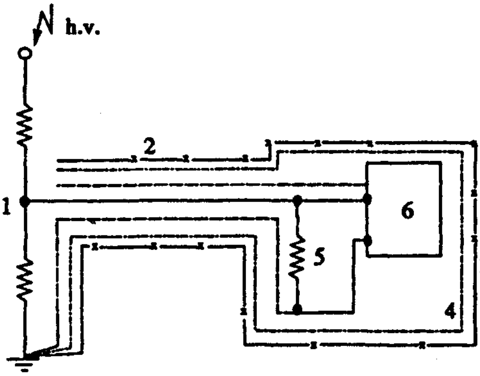

1. Potential divider
2. Triple shielded cable
3. Outer shield enclosure
4. Inner shielded enclosure
5. Terminating impedance
6. CRO

Fig. 7.56 Impulse measurements using multiple shield enclosures and signal cable

Another important factor is the layout of power and signal cables in the impulse testing laboratories. Power and interconnecting cables should not be laid in a zig-zag manner and should not be cross connected. All power cables and control cables have to be arranged through earthed and shielded conduits. A typical schematic layout is shown in Fig. 7.57. The arrangement should provide for branched wiring from the cable tree and should not form loops. Where environmental conditions are so severe that true signal cannot be obtained with all countermeasures, electro-optical techniques for transmitting signal pulses may have to be used.

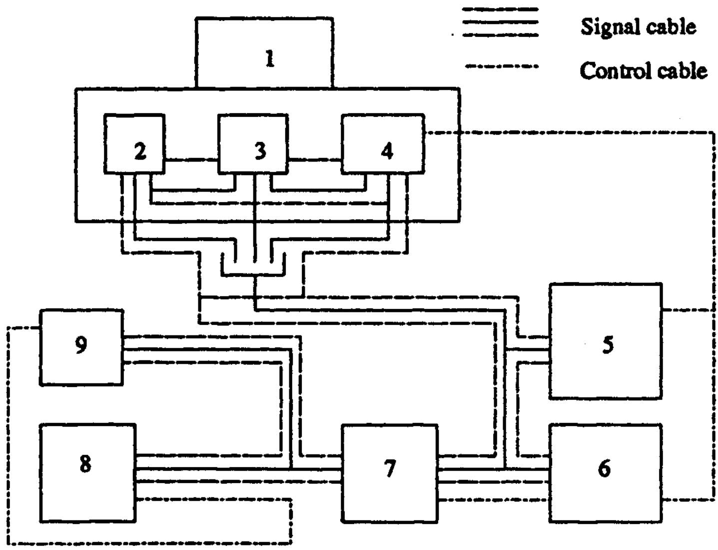

1. Control room
2. Peak reading meter
3. Oscillograph
4. Control centre
5. Rectifier for impulse generator
6. Impulse generator
7. Voltage divider
8. Test object
9. Sphere gap

Fig. 7.57 Layout of an impulse testing laboratory with control and signal cables

QUESTIONS

Q.7.1 Discuss the different methods of measuring high d.c. voltages. What are the limitations in each method ?

Q.7.2 Describe the generating voltmeter used for measuring high d.c. voltages. How does it compare with a potential divider for measuring high d.c. voltages ?

Q.7.3 Compare the relative advantages and disadvantages of using a series resistance microammeter and a potential divider with an electrostatic voltmeter for measuring high d.c. voltages ?

Q.7.4 Why are capacitance voltage dividers preferred for high a.c. voltage measurements ?

Q.7.5 What is capacitance voltage transformer ? Explain with phasor diagram how a tuned capacitance voltage transformer can be used for voltage measurements in power systems.

Q.7.6 Explain the principle and construction of an electrostatic voltmeter for very high voltages. What are its merits and demerits for high voltage a.c. measurements ?

Q.7.7 Give the basic circuit for measuring the peak voltage of (a) a.c. voltage, and (b) impulse voltage. What is the difference in measurement technique in the above two cases ?

Q.7.8 Explain how a sphere gap can be used to measure the peak value of voltages. What are the parameters and factors that influence such voltage measurement ?

Q.7.9 Compare the use of uniform field electrode spark gap and sphere gap for measuring peak values of voltages.

Q.7.10 What are the conditions to be satisfied by a potential divider to be used for impulse work ?

Q.7.11 Give the schematic arrangement of an impulse potential divider with an oscilloscope connected for measuring impulse voltages. Explain the arrangement used to minimise errors.

Q.7.12 What is a mixed potential divider ? How is it used for impulse voltage measurements ?

Q.7.13 Explain the different methods of high current measurements with their relative merits and demerits.

Q.7.14 What are the different types of resistive shunts used for impulse current measurements ? Discuss their characteristics and limitations.

Q.7.15 What are the requirements of an oscillograph for impulse and high frequency measurements in high voltage test circuits ?

Q.7.16 Explain the necessity of earthing and shielding arrangements in impulse measurements and in high voltage laboratories. Give a sketch of the multiple shielding arrangements used for impulse voltage and current measurements.

Q.7.17 A generating voltmeter is to read 250 kV with an indicating meter having a range of (0 – 20) μA calibrated accordingly. Calculate the capacitance of the generating voltmeter when the driving motor rotates at a constant speed of 1500 r.p.m.

Q.7.18 The effective diameter of the moving disc of an electrostatic voltmeter is 15 cm with an electrode separation of 1.5 cm. Find the weight in gms that is necessary to be added to balance the moving plate when measuring a voltage of 50 kV d.c. Derive the formula used. What is the force of attraction between the two plates when they are balanced ?

Q.7.19 A compensated resistance divider has its high voltage arm consisting of a series of resistance whose total value is 25 kilo-ohms shunted by a capacitance of 400 pF. The L.V. arm has a resistance of 75 ohms. Calculate the capacitance needed for the compensation of this divider.

Q.7.20 What are the usual sources of errors in measuring high impulse voltages by resistance potential dividers? How are they eliminated? An impulse resistance divider has a high voltage arm with a 5000 ohm resistance and the L.V. arm with a 5 ohm resistance. If the oscilloscope is connected to the secondary arm through a cable of surge impedance 75 ohms, determine, (i) the terminating resistance, and (ii) the effective voltage ratio.

Q.7.21 A mixed *R-C* divider has its h.v. arm consisting of a capacitance of 400 pF in series with a resistance of 100 ohms. The L.V. arm has a resistance of 0.175 ohm in series with a capacitance C_2. What should be the L.V. arm capacitance for correct compensation? The divider is connected to a CRO through a measuring cable of 75 ohms surge impedance. What should be the values of R_4 and C_4 (see Fig. 7.38(b)) in the matching impedance? Determine the voltage ratio of the divider.

WORKED EXAMPLES

Example 7.1: A generating voltmeter has to be designed so that it can have a range from 20 to 200 kV d.c. If the indicating meter reads a minimum current of 2 μA and maximum current of 25 μA, what should the capacitance of the generating voltmeter be ?

Solution: Assume that the driving motor has a synchronous speed of 1500 rpm.

$$I_{rms} = \frac{VC_m}{\sqrt{2}}\omega$$

where,

V = applied voltage,

C_m = capacitance of the meter, and

ω = angular speed of the drive

Substituting,

$$2 \times 10^{-6} = \frac{20 \times 10^3 \times C_m}{\sqrt{2}} \times \frac{1500}{60} \times 2\pi$$

$$\therefore \quad C_m = 0.9 \text{ p.F}$$

At

$$200 \text{ kV}, I_{rms} = \frac{200 \times 10^3 \times 0.9 \times 10^{-12} \times 1500}{\sqrt{2} \times 60} 2\pi$$

$$= 20.0\ \mu\text{A}$$

The capacitance of the meter should be 0.9 pF. The meter will indicate 20 kV at a current 2 μA and 200 kV at a current of 20 μA.

Example 7.2: Design a peak reading voltmeter along with a suitable micro-ammeter such that it will be able to read voltages, up to 100 kV (peak). The capacitance potential divider available is of the ratio 1000 : 1.

Solution: Let the peak reading voltmeter be of the Haefely type shown in Fig. 7.17a.

Let the micro-ammeter have the range 0 – 10 μA.

The voltage available at the C_2 arm $= 100 \times 10^3 \times \frac{1}{1000}$

$$= 100 \text{ V (peak)}$$

The series resistance R in series with the micro ammeter

$$= \frac{100}{10 \times 10^{-6}}$$

$$= 10^7 \Omega$$

$C_S R$ = 1 to 10 s

Taking the higher value of 10 s, $C_S = \frac{10}{10^7}$

$$= 1\ \mu\text{F}$$

The values of C_S and R are 1 μF and $10^7 \Omega$.

Example 7.3: Calculate the correction factors for atmospheric conditions, if the laboratory temperature is 37°C, the atmospheric pressure is 750 mm Hg, and the wet bulb temperature is 27°C.

Solution: Air density factor, $d = \frac{p}{760} \frac{293}{(273 + t)}$

At $t = 37$°C $\quad d = \frac{750}{760} \frac{293}{310}$

$= 0.9327$

From Table 7.6 air density correction factor $K = 0.9362$. From Fig. 10.1, the absolute humidity (by extrapolation) corresponding to the given temperature is 18 g/m^3. From Fig. 10.2, the humidity correction factor for 50 Hz (curve *a*) is 0.925.

(Note: No humidity correction is needed for sphere gaps.)

Example 7.4: A resistance divider of 1400 kV (impulse) has a high voltage arm of 16 kilo-ohms and a low voltage arm consisting 16 members of 250 ohms, 2 watt resistors in parallel. The divider is connected to a CRO through a cable of surge impedance 75 ohms and is terminated at the other end through a 75 ohm resistor. Calculate the exact divider ratio.

Solution: h.v. arm resistance, $R_1 = 16{,}000$ ohms

l.v. arm resistance, $\quad R_2 = \frac{250}{16}$ ohms

Terminating resistance, $\quad R_2' = 75$ ohms

hence, the divider ratio, $\quad a = 1 + R_1/R_2 + R_1/R_2'$

$= 1 + 16{,}000 \times 16/250$

$= 1 + 16{,}000/75$

$= 1 + 1024 + 213.3 = 1238.3$

Example 7.5: The H. V. arm of an *R-C*, divider has 15 numbers of 120 ohm resistors with a 20 pF capacitor to ground from each of the junction points. The L.V. arm resistance is 5 ohms. Determine the capacitance needed in the L.V. arm for correct compensation.

Solution: Ground capacitance per unit $= C_g' = 20$ pF

Effective ground capacitance $= C_e = (2/3)\, C_g$

$= 2/3\,(15 \times 20)$

(Refer Fig. 7.34)

$= 200$ pF

This capacitance is assumed to be between the center tap of the H.V. arm and the ground as shown in Fig. 7.28.

Here, $\quad R_1/2 = 15 \times 120/2 = 900$ ohms

$R_2 = 5$ ohms.

Then, the effective time constant of the divider,

$= (R_1/2 \cdot (2/3)\, C_g) = R_1 C_e/2$

$$= ((900 \times 200 \times 10^{-12})/2s = 90 \text{ n s}$$

Making the L.V. arm time constant to be the same as that of the H.V arm; the capacitance required for compensation is calculated as:

$$R_2C_2 = 90 \text{ n sec.}$$

$$C_2 = 90/5 \text{ nF} = 18 \times 10^{-9}\text{F}$$

Example 7.6: A coaxial shunt is to be designed to measure an impulse current of 50 kA. If the bandwidth of the shunt is to be at least 10 MHz and if the voltage drop across the shunt should not exceed 50 V, find the ohmic value of the shunt and its dimensions.

Solution: Resistance of the shunt (max) $R = \dfrac{50}{50 \times 10^2}$

$$= 1 \text{ m}\Omega$$

Taking the simplified equivalent circuit of the shunt as given in Fig. 7.48(b)

Bandwidth $B = \dfrac{1.46R}{L_0} = 10 \text{ MHz}$

or, $L_0 = \dfrac{1.46R}{B} = \dfrac{1.46 \times 10^{-2}}{10 \times 10^6}$

$$= 1.46 \times 10^{-10} \text{ H}$$

or 0.146 n H

d, the thickness of the cylindrical resistive tube is taken from the consideration of the bandwidth as

$$B = \frac{1.46\rho}{\mu d^2}$$

where,

ρ = resistivity of the material,

$\mu = \mu_0 = 4\pi \times 10^{-7}$ H/m, and

d = thickness of the tube in metres

Let r = radius of the resistive tube,

l = length of the resistive tube,

d = thickness of the resistive tube, and

ρ = resistivity of the tube material.

Then the bandwidth $B = \dfrac{1.46\rho}{\mu d^2}$

where, $\mu = \mu_0\mu_r \approx \mu_0$

Substituting $B = 10^7$ Hz

$\rho = 30 \times 10^{-8}$ Ωm

$$\mu_0 = 4\mu \times 10^{-7}$$

$$d = \sqrt{\frac{1.46\rho}{\mu B}}$$

$$= \sqrt{\frac{1.46 \times 30 \times 10^{-8}}{4\pi \times 10^{-7} \times 10^7}}$$

$$= 0.187 \times 10^{-8}\ \text{m}$$

$$= 0.187\ \text{mm}$$

Let the length l be taken as 10 cm or 10^{-1} m;

then, $$R = \frac{\rho l}{A} = \frac{\rho l}{(2\pi r)d} = 1\ \text{m}\Omega$$

or, $$r = \frac{\rho l}{2\pi R d}$$

$$= \frac{30 \times 10^{-8} \times 10^{-1}}{2\pi \times 10^{-3} \times 0.187 \times 10^{-3}}$$

$$= 25.5 \times 10^{-3}\ \text{m}$$

or 25.5 mm.

For the return conductor the outer tube can be taken to have a length = 10 cm, radius = 30 mm, and thickness = 1 mm, and it can be made from copper or brass.

Example 7.7: A Rogowski coil is to be designed to measure impulse currents of 10 kA having a rate of change of current of 10^{11} A/s. The current is read by a VTVM as a potential drop across the integrating circuit connected to the secondary. Estimate the values of mutual inductance, resistance, and capacitance to be connected, if the meter reading is to be 10 V for full-scale deflection.

Solution: $V_m(t) = \frac{M}{CR} I(t)$ for $\frac{1}{CR} << \omega$ (Eq. 7.42),

taking the peak values

$$\frac{M}{CR} = \frac{V_m(t)}{I(t)} = \frac{10}{10^4} = 10^{-3}$$

The time interval of the change of current assuming sinusoidal variation is

$$\frac{10^4}{10^{11}} = 10^{-7}\ \text{s} = \frac{1}{4}\ \text{of a cycle}$$

$\therefore$ frequency $$= \frac{10^7}{4}\ \text{Hz}$$

and, $$\omega = 2\pi f = \frac{\pi}{2} \times 10^7$$

Taking $$\frac{1}{CR} = \frac{\omega}{10\pi} = \frac{10^6}{2}$$

$$CR = \frac{2}{10^6}$$

$$M = 10^{-3}CR = 10^{-3}\frac{2}{10^6}$$

$$= 2\times10^{-9}\text{ H or } 2\text{ n H.}$$

Taking $R = 2\times10^3\ \Omega$,

$$C = \frac{CR}{R} = 2\times10^{-6}/20\times\ 10^2$$

$$= 10^{-9}\text{ F or } 1000\text{ pF}$$

(It should be noted that for a given frequency, $X_c << R$; otherwise the low frequency response will be poor. Here X_c at $f = 10^7/4$ is 60Ω only.)

Example 7.8: If the coil in Example 7.7 is to be used for measuring impulse current of 8/20 μ s wave and of the same peak current, what should be the R-C integrating circuit.

Solution: In this case, the lowest frequency to be read should be at least $\frac{1}{3}$ to $\frac{1}{5}$ of the lowest frequency component present in the waveform.

The frequency corresponding to the tail time is

$$\frac{1}{20\times\ 10^{-6}} = 50\text{ kHz}$$

∴ lowest frequency to be read is

$$50\times\frac{1}{5} = 10\text{ kHz}$$

$$\therefore\ \omega = 2\pi\times10^4\text{ radians}$$

Taking
$$\frac{1}{CR} = \frac{\omega}{10\pi}$$

$$= \frac{2\pi\times10^4}{10\pi} = 2\times10^3$$

$$M = 10^{-3}\times\frac{1}{2\times\ 10^3} = 0.5\times10^{-6}\text{ H, or } 0.5\ \mu\text{H}$$

Taking
$$R = 2\times10^3\Omega\text{ as before,}$$

$$C = \frac{0.5\times\ 10^{-3}}{2\times\ 10^3}$$

$$= 0.25\ \mu\text{F}$$

(X_c at a frequency of 10 kHz is about 60Ω which is very much less than R.)

REFERENCES

1. Craggs, J.D. and Meek, J.M., *High Voltage Laboratory Techniques*, Butterworths Scientific Publications, London (1964).
2. Kuffel, E., and Abdullah, M., *High Voltage Engineering*, Pergamon Press, Oxford (1970).
3. Schwab, A.J., *High Voltage Measurement Technique*, M.I.T. Press, Cambridge, Massachusetts (1972).
4. Bowlder, G.W., *Measurement in High Voltage Test Circuits*, Pergamon Press, Oxford (1975).
5. Begamudre, R.D., "*E.H.V. A.C. Transmission Engineering*, Wiley Eastern, New Delhi (1986).
6. Hylten Cavallius, N., *High Voltage Laboratory Planning*, Haefely and Co., Basel, Switzerland (1988).
7. "Method of voltage measurement by means of sphere gaps (one sphere earthed)" *IS* : 1876-1961.
8. "Methods of impulse voltage testing", *IS : 2070-1962.*
9. "Methods of high voltage testing", *IS : 2071-1962.*
10. "On sphere gap measurements", *BS : 358-1960.*
11. "Recommendations for voltage measurements by sphere gaps", *IEC Publication No. 52-1960.*
12. Trump, G.J. and Van De Graaff *et al.*, "Generator voltmeter of high voltage sources", *Rev. Sci. Instr.*, **11**, 54 (1940).
13. Hamwell and Van Voorhis, "An electrostatic generating voltmeter", *Rev. Sci. Instr.*, **4**, 540 (1933).
14. Kuffel, E., "The influence of nearby earth objects and polarity of voltage on d.c. breakdown of sphere gaps", *Proc. IEE, Part A*, **108**, 302 (1961).
15. Kuffel, E., "The effect of irradiation on breakdown voltage of sphere gaps in air under d.c. and a.c. voltages", *Proc. IEE, Part C*, **106**, 133 (1956).
16. Davis *et al.*, "Measurement of high voltages with special reference to peak voltages", *Proc. IEE*, **68**, 1222 (1930).
17. Spharpe *et al.*, "Crest voltmeters", *Tr. AIEE*, **35**, 99 (1916).
18. Rabus, W., "Peak voltmeters", *Z. Elektrot*, **3**, 7 (1950).
19. Haefely and Co., "*H.V. meter for peak and rms value measurements*", Druckschirf, BD., 6589 Basel (1967).
20. Rabus, W., "Measurements of surges by V.T.V.M. and electrostatic voltmeters", *ETZ(A)*, **75**, 6761 (1953).
21. Blalock *et al.*, "A capacitive voltage divider for UHV outdoor testing", *Tr. IEEE PAS*, **PAS-89**, 1404 (1970).
22. Ziegler, "Highly stable 150 kV voltage divider", *Tr. IEEEIM*, **IM-19**, 395 (1970).
23. High voltage testing techniques, *IEC Publication No. 60-1962.*
24. Koshrt, F., "Hall generators for high d.c. current measurements", *ETZ* (*A*), **77**, 487 (1956).
25. Thomas, R.F., "Fast light pulse measuring schemes", *Tr. IEEEIM*, **IM-17**, 12 (1968).
26. Mckibbin, F., "Use of delta modulation in pulse transmission system", *EE Trans.*, **6**, 55 (1970).
28. Witt, R., "Response of low resistance shunts for impulse currents", *Eleteckric*, **47**, 54 (1960).
29. Schwab, A., "Low ohmic resistors for impulse currents", *Transaction 12, of H.V. Laboratory*, University of Karlsruhe, 1972.

30. Schwab, A., *ETZ(A)*, **87**, 181 (1966).
31. Heumann, K., "Magnetic potentiometer of high precision", *Tr. IEEEIM*, **IM-15**, 242 (1966).
32. Ficchi, R.C., *Electrical interference*, McGraw-Hill, New York (1963).
33. Thomas, R.T. *et al.*, "High impulse current and voltage measurements", *Tr. IEEE IM*, **IM-19**, 102 (1970).
34. Cassidy, E.C. *et al.*, "Electro-optical H.V. pulse measurement techniques", *Tr. IEEE IM*, **IM-19**, 395 (1970).
35. Zaengel, W., "Impulse voltage dividers and leads", *Bull, SEV*, **61**, 1003 (1970).
36. Faser, K., "Transient behaviour of damped capacitive voltage dividers of million-volts", *Tr.IEEE PAS*, **93**.116 (1974).
37. Hylten Cavallius, N., et al., "A new approach to minimise response errors in the measurement of high voltages", *Tr. IEEE PAS, Vol. PAS-102, 2077* (1983).
38. Hylten Cavallius, N., et al., "Response errors of shunts", *Int. Symp. on High Voltage Engineering, Paper No. 61.05*, Athens, Greece (1983).